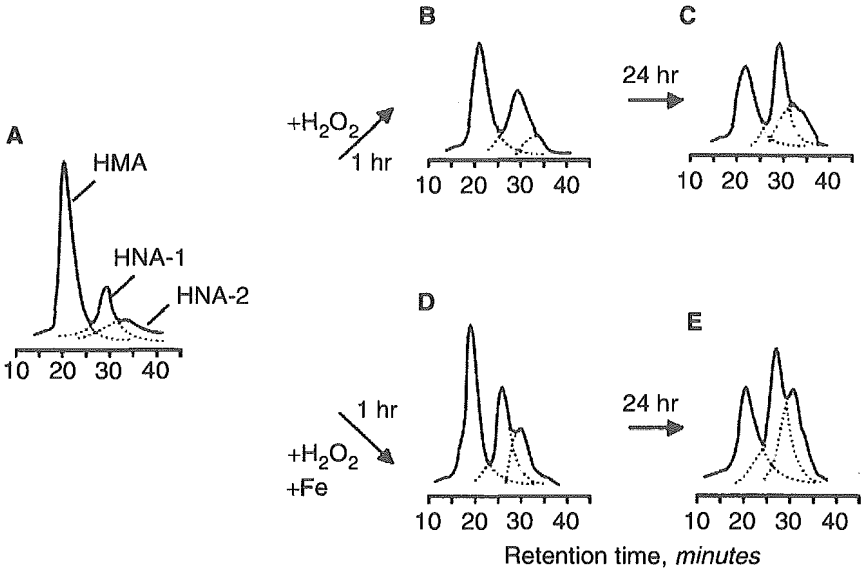


**Fig. 1. High-performance liquid chromatography (HPLC) profile of in vitro–oxidized serum albumin.** HPLC profile of albumin from a normal subject under basal condition (*A*). Serum was incubated with 200 μmol/L of $H_2O_2$ in the presence or absence of 180 μmol/L of saccharated ferric oxide for 1 hour (*B* and *D*) or 24 hours (*C* and *E*). Five-μL aliquots of each serum were analyzed by HPLC using a Shodex Asahipak ES-502N column. HMA; mercaptalbumin (reduced form), HNA-1; nonmercaptalbumin (disulfide form), HNA-2; nonmercaptalbumin (oxidized form).

For each experiment, the carbonyl density was determined from the blot with the shortest possible exposure time required to produce clearly visible bands. DNP and protein blots were scanned using the same size section of the blot for each scan. The uniform window size and analysis box ensured that data were being analyzed consistently from band to band and from blot to blot. Because the concentration of various plasma proteins differs between patient groups and healthy subjects, densitometry data for the area of the DNP blot band were divided by the densitometry data for the area of the protein blot band obtained under identical gel loading and electrotransfer conditions. These data are recorded as DNP area/protein area and are reported in densitometry units. The mean for each subject group was calculated from each blot.

### Statistics

Statistical significance was evaluated using the two-tailed, unpaired Student *t* test for comparisons between two means, or analysis of variance (ANOVA) analysis followed by Newman-Keuls method for more than two means. A value of $P < 0.05$ was regarded as statistically significant. Results are reported as mean ± SE.

## RESULTS

### Oxidation of serum albumin by $H_2O_2$ and Fe in vitro

The current study was designed to determine the redox state of HD patients, and to examine the effect of IVIR on oxidative stress, especially oxidation of serum albumin, in HD patients. First of all, we determined the HPLC profile of serum albumin before and after in vitro oxidation by $H_2O_2$ and Fe treatment. HPLC analysis allowed us to determine the oxidation status of Cys-34 residues in the albumin. Sera from healthy subjects were incubated with 200 μmol/L of $H_2O_2$ with or without 180 μmol/L of saccharated ferric oxide for 1 hour or 24 hours, and then subjected to HPLC analysis as described in the **Methods** section. Figure 1 shows typical HPLC profiles of serum albumin from a healthy volunteer before and after oxidation treatment. Serum albumin is separated into three peaks by the HPLC column (Fig. 1A). The first peak represents HMA (reduced form), the second peak, HNA-1 (disulfide form; HNA(Cys) or HNA(Glut)), and the third peak HNA-2 (oxidized from; HNA(Oxi)). Treatment of serum with 200 μmol/L of $H_2O_2$ for 1 hour resulted in a slight increase in HNA-1 and almost no change in HNA-2 (Fig. 1B). Twenty-four hours after incubation, HMA was reduced and both HNA-1 and HNA-2 fractions were further increased, indicating the oxidation of Cys-34 residues in the albumin (Fig. 1C). In the presence of 180 μmol/L of saccharated ferric oxide, treatment of serum with 200 μmol/L of $H_2O_2$ further potentiated the oxidation of albumin both at 1 and 24 hours (Fig. 1D and E). The ratio of each albumin fraction to the total albumin (f(HMA), f(HNA-1), and f(HNA-2)) was calculated, and those data are summarized in Table 1. As shown in Table 1, incubation of serum with 200 μmol/L of $H_2O_2$ and 10 μg/mL of saccharated ferric oxide for 24 hours markedly increased f(HNA-1) and f(HNA-2) values when compared with those with $H_2O_2$ treatment alone ($P < 0.05$). These results suggest that treatment with saccharated ferric oxide could enhance the oxidation of serum albumin in the presence of $H_2O_2$, and that HPLC analysis of serum albumin provides quantitative and qualitative values for the oxidation status of albumin.

### Oxidation of serum albumin in HD patients

Next, we determined the oxidation status of serum albumin by HPLC analysis from HD patients with or

**Table 1.** f(HMA), f(HNA-1), and f(HNA-2) values (%) for reduced and oxidized albumin in serum from normal subjects treated with $H_2O_2$ in the presence or absence of saccharated ferric oxide

| | | Without saccharated ferric oxide | | | With saccharated ferric oxide | | |
|---|---|---|---|---|---|---|---|
| | | 0 hr | 1 hr | 24 hrs | 0 hr | 1 hr | 24 hrs |
| | f(HMA) | 69.5 ± 0.2 | 67.3 ± 0.7 | 45.9 ± 1.1 | 69.9 ± 3.5 | 62.3 ± 0.8 | 44.9 ± 0.8 |
| $H_2O_2$ | f(HNA-1) | 24.9 ± 0.7 | 26.6 ± 1.6 | 35.0 ± 1.4 | 23.0 ± 0.5 | 27.7 ± 0.6 | 45.5 ± 0.4[a] |
| (200 μ mol/L) | f(HNA-2) | 5.6 ± 0.9 | 6.1 ± 1.7 | 8.5 ± 2.5 | 7.1 ± 2.0 | 9.7 ± 0.2 | 13.6 ± 1.1[a] |

[a] $P < 0.05$ as compared with serum treated with $H_2O_2$ in the absence of saccharated ferric oxide. Values are expressed as mean ± SE ($N = 4$).

**Table 2.** f(HMA), f(HNA-1), and f(HNA-2) values (%) for reduced and oxidized albumin in serum from normal subjects and patients without IVIR treated with vehicle or saccharated ferric oxide

| | Healthy subjects | | Patients without IVIR | |
|---|---|---|---|---|
| | Vehicle | Saccharated ferric oxide | Vehicle | Saccharated ferric oxide |
| f(HMA) | 66.7 ± 0.7 | 64.6 ± 0.4 | 45.4 ± 2.1 | 36.9 ± 1.0[a] |
| f(HNA-1) | 27.8 ± 0.6 | 29.7 ± 0.5 | 41.3 ± 2.3 | 43.6 ± 1.6 |
| f(HNA-2) | 5.5 ± 0.1 | 5.6 ± 0.2 | 13.3 ± 0.6 | 19.5 ± 1.5[a] |

[a] $P < 0.05$ as compared with serum treated with vehicle. Values are expressed as mean ± SE ($N = 7$).

without IVIR, as well as from healthy subjects, because albumin is the most abundant serum protein and has been shown to be a target of oxidative stress in uremic patients. Patient profiles of healthy subject group, IVIR group, and no-IVIR group are summarized in Table 2. Data in the patients group were obtained after the treatment period. Parameters for iron status were examined before and after IVIR. Patient groups did not differ in respect to age, gender, diabetes/nondiabetes ratio, duration and efficacy of dialysis, serum albumin, uric acid, and C-reactive protein (CRP) levels. Serum Fe and TSAT levels in HD patients with IVIR were slightly, but not significantly, higher than in those without IVIR, and serum ferritin levels were significantly increased in IVIR group due to iron administration ($P < 0.05$). Figure 2 shows typical HPLC profiles for serum albumin from healthy subjects (Fig. 2A), HD patients without IVIR (Fig. 2B), and with IVIR (Fig. 2C). The ratio of each albumin fraction to the total albumin (f(HMA), f(HNA-1), and f(HNA-2)) was calculated and those data are summarized in Table 3. As shown in Figure 2 and Table 3, f(HMA) was substantially decreased and both f(HNA-1) and f(HNA-2) were significantly increased in HD patients compared with healthy subjects ($P < 0.05$). IVIR treatment resulted in marked increases in both f(HNA-1) and f(HNA-2) in HD patients ($P < 0.05$), while there was no significant change in f(HMA). These findings suggest that Cys-34 residue in albumin is highly oxidized in HD patients and that IVIR resulted in the overoxidation of albumin. In order to determine the relationship between the redox status of plasma proteins and the Cys-34 oxidation of serum albumin, as detected by HPLC, the plasma protein carbonyl contents of these patients were also determined.

### Plasma protein carbonyl contents in HD patients

In most cases, protein oxidation is associated with an increase in carbonyl content. It is known that an increase in carbonyl contents reflects the oxidation of Lys, Arg, or Pro residues in a protein. Plasma protein carbonyl contents were significantly increased in HD patients, and IVIR further enhanced the carbonylation of plasma protein (IVIR: 2.2 ± 0.4 nmol/mg protein, $N = 11$; no IVIR: 1.0 ± 0.1 nmol/mg protein, $N = 11$; healthy subjects: 0.4 ± 0.03 nmol/mg protein, $N = 11$, $P < 0.05$). We next determined the carbonyl contents of major plasma proteins separately by Western blot analysis using an anti-DNP antibody. Figure 3A shows a representative blot and Figure 3B summarizes results obtained from the multiple blots. Interestingly, only albumin was significantly oxidized in HD patients, and IVIR increased the albumin oxidation ($P < 0.05$). There was no statistically significant difference in the carbonyl contents of other plasma proteins such as transferrin, immunoglobulin, and fibrinogen among three groups (healthy subjects, HD patients without IVIR, and HD patients with IVIR). These findings suggest that the origin of the increase in plasma protein carbonyl contents in HD patients was largely from an increase in oxidized albumin, and that IVIR substantially increased plasma protein carbonyl contents by oxidizing albumin.

### Relationship between HPLC profile of albumin and plasma protein carbonyl content

In order to validate the usefulness of HPLC analysis of serum albumin for the assessment of oxidative stress in HD patients, we determined the relationship between plasma protein carbonyl contents and f(HNA-1) or f(HNA-2) values because plasma protein carbonyl contents are one of the reliable and widely used oxidative stress markers. As shown in Figure 4, both f(HNA-1) and f(HNA-2) have strong correlation with plasma protein carbonyl contents ($R = 0.674$ and $R = 0.724$, respectively, $P < 0.01$). We also investigated the relationship between AOPP levels and f(HNA-1) or f(HNA-2) values, and obtained significant correlation (data not shown). These findings suggest the possibility that f(HNA-2) values can be useful markers for the evaluation of redox status of HD patients.

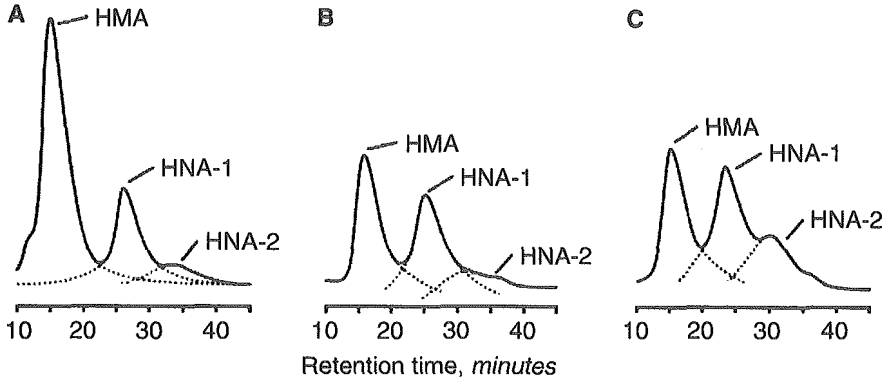


**Fig. 2. High-performance liquid chromatography (HPLC) profile of serum albumin from HD patients with or without intravenous iron administration (IVIR).** Five-μL aliquots of serum from HD patients with or without IVIR, and healthy subjects were subjected to HPLC analysis using a Shodex Asahipak ES-502N column. A representative tracing of HPLC profiles of serum albumin from normal subjects (*A*). A representative tracing of HPLC profiles of serum albumin from HD patients without IVIR (*B*). A representative tracing of HPLC profile of serum albumin from patients treated with IVIR (*C*).

**Table 3.** Characteristics of patient group

| | Healthy subjects ($N = 11$) | Patients without IVIR ($N = 11$) | | Patients with IVIR ($N = 11$) | |
|---|---|---|---|---|---|
| | | After vehicle | Before vehicle | After IVIR | Before IVIR |
| Age *years* | 67.7 ± 0.4 | 68.0 ± 3.7 | | 68.6 ± 5.6 | |
| Gender *M/F* | 7/4 | 8/3 | | 7/4 | |
| Duration of dialysis *months* | – | 22.4 ± 7.5 | | 22.5 ± 7.1 | |
| Diabetes/nondiabetes | – | 5/6 | | 4/7 | |
| Kt/Vurea | – | 1.46 ± 0.04 | | 1.52 ± 0.08 | |
| Albumin *g/dL* | 4.27 ± 0.07 | 3.73 ± 0.11 | | 3.53 ± 0.14 | |
| Uric acid *mg/dL* | 4.79 ± 0.3 | 8.1 ± 0.6 | | 7.8 ± 0.4 | |
| CRP *mg/dL* | 0.15 ± 0.04 | 0.28 ± 0.06 | | 0.27 ± 0.08 | |
| Fe μg/*dL* | 83.82 ± 5.55 | 47.6 ± 6.5 | 49.4 ± 5.8 | 55.4 ± 2.6 | 45.5 ± 4.4 |
| TSAT % | 28.97 ± 2.61 | 23.0 ± 6.7 | 21.2 ± 8.7 | 28.6 ± 6.2 | 21.0 ± 1.7 |
| Ferritin *ng/mL* | 43.27 ± 4.99 | 96.9 ± 19.1 | 102.5 ± 24.3 | 231.4 ± 55.4[a] | 75.4 ± 16.2 |

[a] $P < 0.05$. Values are expressed as mean ± SE.

## DISCUSSION

The current studies demonstrate that serum albumin is highly oxidized in HD patients, with an increase in the disulfide form, and that IVIR on these patients significantly increased the oxidation status of albumin, as evidenced by a marked increase in the oxidized form. To our knowledge, this is the first report demonstrating the effect of IVIR on the oxidation of serum albumin in HD patients. Plasma is known to contain a wide range of important antioxidants, including albumin, ascorbate, and urate. In contrast, the concentrations of superoxide dismutase, reduced glutathione, and catalase, all of which are known to be important intracellular antioxidants, are low in the plasma and are not likely to serve as important plasma antioxidants [25, 26]. It has previously been established that certain amino acid residues of proteins are particularly susceptible to free radical attack [27, 28], and several studies have confirmed that Cys-34 of serum albumin is highly accessible to reactive oxygen species such as $H_2O_2$ [29, 30] and carbon-centered free radicals [31], as well as other oxidizing agents, such as nitric oxide (NO) [32–34] and peroxynitrite ($ONOO^-$) [29, 35]. In addition, it has been demonstrated that Cys-34 of oxidized albumin is further oxidized to sulfenic, sulfinic, or sulfonic state under stronger $H_2O_2$-mediated [29, 30] and anaerobic NO–mediated [33] oxidizing conditions. In plasma, free thiol groups are quantitatively the most important scavengers of oxidants, and are known to be largely located on the albumin molecule. Furthermore, we confirmed the carbonyl formation of plasma albumin, as previously demonstrated by Himmelfarb et al [3], suggesting that basic amino acid residues in albumin as well as Cys-34 are also oxidized. Because albumin is the most abundant plasma protein, it could play a major role as an antioxidant in plasma at least by thiol oxidation and carbonyl formation. We recently demonstrated that the plasma half-life of radiolabelled- and in vitro oxidized-albumin was substantially decreased in mice, and that the liver uptake clearance of oxidized albumin was markedly increased by 11-fold [36]. These findings suggest that serum albumin might play an important protective role against reactive free radicals in extracellular fluids via its oxidation and the subsequent clearance from the systemic circulation by the liver. In this context, we expected that the characterization of oxidation status of serum albumin might provide useful information regarding the redox state of the human body, prompting us to examine the effect of IVIR on the oxidation of albumin. As shown

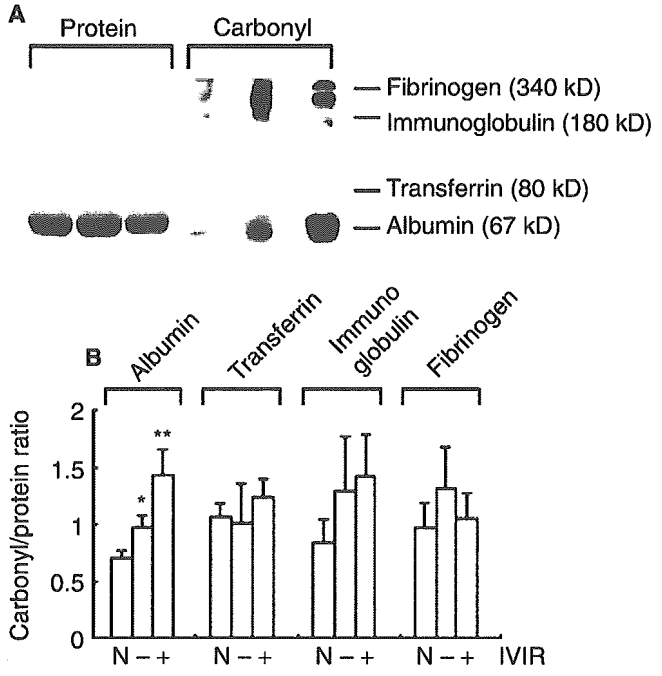


**Fig. 3. Carbonyl content of major plasma proteins from normal subjects and HD patients with or without intravenous iron administration (IVIR).** Plasma samples from HD patients with or without IVIR were derivatized with DNP and subjected to duplicate SDS-PAGE gels (*A*). Following electrotransfer, one blot was stained with Coomassie brilliant blue G for protein (upper blot) and the second blot was stained for DNP using OxiBlot kit reagents (lower blot). Carbonyl formation of major plasma proteins (albumin, transferrin, immunoglobulin, and fibrinogen) were determined as densitometry ratio of DNP area and protein area, and are reported in densitometry units (*B*). Values are expressed as mean ± SE; $N = 11$ patients per group. $^{*}P < 0.05$ as compared with plasma from patients without IVIR.

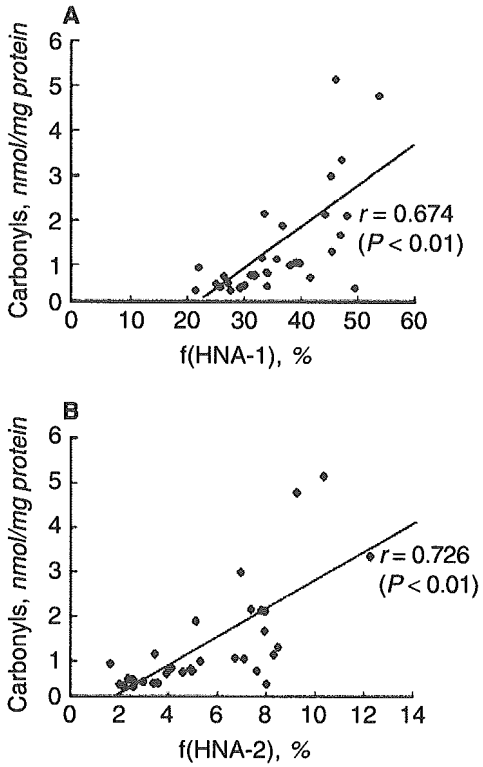


**Fig. 4. Relationship between plasma protein carbonyl content and f(HNA-1) (*A*) or f(HNA-2) (*B*).** Plasma protein carbonyl contents and f(HNA-1) or f(HNA-2) values from normal subjects and HD patients with or without intravenous iron administration (IVIR) are plotted, and the line shows linear regression of plasma protein carbonyl content and f(HNA-1) or f(HNA-2) values ($N = 33$, $R = 0.674$ and $R = 0.724$, respectively, $P < 0.01$).

**Table 4.** f(HMA), f(HNA-1), and f(HNA-2) values (%) for reduced and oxidized albumin in sera from healthy subjects and HD patients with or without IVIR

| | Healthy subjects ($N = 11$) | Patients without IVIR ($N = 11$) | Patients with IVIR ($N = 11$) |
|---|---|---|---|
| f(HMA) | 68.1 ± 2.12 | 58.5 ± 7.37[a] | 50.3 ± 7.25[a] |
| f(HNA-1) | 28.9 ± 1.76 | 36.0 ± 6.03[a] | 41.7 ± 6.27[a,b] |
| f(HNA-2) | 2.99 ± 0.40 | 5.46 ± 1.50[a] | 8.7 ± 2.22[a,b] |

Values are expressed as mean ± SE.
[a] $P < 0.05$ as compared with sera from healthy subjects.
[b] $P < 0.05$ as compared with sera from patients without IVIR.

in Figure 1, an HPLC analysis of serum albumin showed a clear separation of HMA, HNA-1, and HNA-2. In HD patients, we found that serum albumin is oxidized, leading to an increase in both f(HNA-1) and f(HNA-2), and that an increase in f(HNA-2) is associated with IVIR. There was no significant difference between the non-IVIR group and IVIR group in several markers that can affect oxidative stress levels, such as dialysis efficiency (Kt/Vurea), uric acid, CRP, and diabetes. These results suggest that HPLC analysis has the potential to provide quantitative as well as qualitative information on the states at oxidation of serum albumin in HD patients. Furthermore, our findings suggest that IVIR is associated with an increase in the oxidized albumin, as evidenced by an increase in f(HNA-2) and plasma protein carbonyl contents.

Cardiovascular diseases continue to be the major cause of both morbidity and mortality for patients on HD therapy. For HD patients, the annual mortality rate caused by cardiovascular disorders is approximately 9%, which is 10- to 20-fold higher than the general population, even when adjusted for age, sex, race, and the presence or absence of diabetes [37]. A potential link between inflammation, hypoalbuminemia, and subsequent cardiovascular risk in HD patients may be through the process of oxidative stress. Although $Fe^{2+}$ is known to be a powerful source of hydroxyl radicals through the Fenton reaction, the majority of HD patients receive IVIR for anemia correction. Because iron loading markedly alters the antioxidant system [38], and because uremic patients have numerous defects in antioxidant defense that are unrelated to iron, iron toxicity could amplify these defects, and IVIR in HD patients may represent a specific condition that enhances iron toxicity through the generation of oxidative stress. This hypothesis is also supported by the

recent study showing that intensive IVIR was an independent factor associated with a decreased survival and higher rates of hospitalization for HD patients [39]. HD patients have relatively lower serum albumin levels for several reasons, including malnutrition. Given the fact that albumin is a major antioxidant in the extracellular fluid, a decrease in serum albumin levels in these patients would contribute to the high incidence of cardiovascular events that are frequently associated with an increase in oxidative stress. Significance of oxidized serum albumin in HD patients in the progression of cardiovascular diseases is not fully determined. However, in the case of HD patients, it has been demonstrated that the carotid artery intima-media thickness is associated with the level of plasma advanced oxidation protein products (AOPP), serum ferritin, and the annual intravenous iron dose administered [40], and that AOPP is mostly due to albumin [41]. These findings suggest the possibility that oxidized albumin in HD patients might play a pathogenic role in the progression of atherosclerosis. A study by Boaz et al has suggested that antioxidant therapy may lessen cardiovascular complications in end-stage renal disease patients [42], suggesting the importance of evaluating oxidative stress and the appropriate antioxidant therapy in HD patients, especially in patients who are receiving IVIR. The coadministration of antioxidants such as vitamin E with IVIR has been shown to be effective in reducing oxidative stress in HD patients [43]. HPLC analysis of serum albumin represents a potentially useful marker for the qualitative and quantitative evaluation of oxidative stress in HD patients, as well as for the assessment of the effect of antioxidant therapy.

## CONCLUSION

The findings here suggest that IVIR is associated with an increase in the oxidative state of serum albumin, and that the HPLC analysis of serum albumin would be a useful marker for the quantitative and qualitative evaluation of oxidative stress in HD patients.

## ACKNOWLEDGMENT

The authors thank Drs. Ken Imanishi, Kenji Machida, Shiho Wakamatsu, Saeko Tajiri (Department of Nephrology, Kumamoto University Graduate School of Medical Sciences, Kumamoto, Japan), and Dr. Motoko Tanaka (Department of Nephrology, Akebono Clinic, Kumamoto, Japan) for blood sample collection from HD patients and for helpful discussions. This work was supported by the Grants-in-Aid for Scientific Research from the Ministry of Education, Culture, Sports, Science and Technology in Japan (13770602 and 15790432 to K.K., 14370759 and 14657618 to M.O., 13877166 and 14370321 to K.T.), and the Salt Science Research Foundation (to K.K.).

*Reprint requests to Kenichiro Kitamura, M.D., Ph.D., Assistant Professor, Department of Nephrology, Kumamoto University Graduate School of Medical Sciences, 1–1-1 Honjo, Kumamoto, Kumamoto 860–8556, Japan.*
*E-mail: ken@gpo.kumamoto-u.ac.jp*

## REFERENCES

1. Descamps-Latscha B, Witko-Sarsat V: Importance of oxidatively modified proteins in chronic renal failure. *Kidney Int* (Suppl 78):S108–S113, 2001
2. Daschner M, Lenhartz H, Botticher D, *et al*: Influence of dialysis on plasma lipid peroxidation products and antioxidant levels. *Kidney Int* 50:1268–1272, 1996
3. Himmelfarb J, McMonagle E: Albumin is the major plasma protein target of oxidant stress in uremia. *Kidney Int* 60:358–363, 2001
4. Lee Y, Shacter E: Role of carbohydrates in oxidative modification of fibrinogen and other plasma proteins. *Arch Biochem Biophys* 321:175–181, 1995
5. Shacter E, Williams JA, Lim M, *et al*: Differential susceptibility of plasma proteins to oxidative modification: Examination by western blot immunoassay. *Free Radic Biol Med* 17:429–437, 1994
6. Sogami M, Nagoka S, Era S, *et al*: Resolution of human mercapt- and nonmercaptalbumin by high-performance liquid chromatography. *Int J Pept Protein Res* 24:96–103, 1984
7. Sogami M, Era S, Nagaoka S, *et al*: HPLC-studies on nonmercapt-mercapt conversion of human serum albumin. *Int J Pept Protein Res* 25:398–402, 1985
8. Peters T, Jr.: *All About Albumin. Biochemistry, Genetics, and Medical Applications*, New York, Academic Press, 1996, pp 9–75
9. Janatova J, Fuller JK, Hunter MJ: The heterogeneity of bovine albumin with respect to sulfhydryl and dimer content. *J Biol Chem* 243:3612–3622, 1968
10. Noel JK, Hunter MJ: Bovine mercaptalbumin and nonmercaptalbumin monomers. Interconversions and structural differences. *J Biol Chem* 247:7391–7406, 1972
11. Wallevik K: SS-interchanged and oxidized isomers of bovine serum albumin separated by isoelectric focusing. *Biochim Biophys Acta* 420:42–56, 1976
12. Hayakawa A, Kuwata K, Era S, *et al*: Alteration of redox state of human serum albumin in patients under anesthesia and invasive surgery. *J Chromatogr B Biomed Sci Appl* 698:27–33, 1997
13. Sogami M, Era S, Nagaoka S, *et al*: High-performance liquid chromatographic studies on non-mercapt in equilibrium with mercapt conversion of human serum albumin. II. *J Chromatogr* 332:19–27, 1985
14. Suzuki E, Yasuda K, Takeda N, *et al*: Increased oxidized form of human serum albumin in patients with diabetes mellitus. *Diabetes Res Clin Pract* 18:153–158, 1992
15. Soejima A, Kaneda F, Manno S, *et al*: Useful markers for detecting decreased serum antioxidant activity in hemodialysis patients. *Am J Kidney Dis* 39:1040–1046, 2002
16. Fishbane S, Maesaka JK: Iron management in end-stage renal disease. *Am J Kidney Dis* 29:319–333, 1997
17. Macdougall IC, Chandler G, Elston O, *et al*: Beneficial effects of adopting an aggressive intravenous iron policy in a hemodialysis unit. *Am J Kidney Dis* 34:S40–S46, 1999
18. Mocks J: Cardiovascular mortality in haemodialysis patients treated with epoetin beta—A retrospective study. *Nephron* 86:455–462, 2000
19. Halliwell B: Superoxide-dependent formation of hydroxyl radicals in the presence of iron salts. Its role in degradation of hyaluronic acid by a superoxide-generating system. *FEBS Lett* 96:238–242, 1978
20. Rooyakkers TM, Stroes ES, Kooistra MP, *et al*: Ferric saccharate induces oxygen radical stress and endothelial dysfunction in vivo. *Eur J Clin Invest* 32(Suppl 1):9–16, 2002
21. Tovbin D, Mazor D, Vorobiov M, *et al*: Induction of protein oxidation by intravenous iron in hemodialysis patients: Role of inflammation. *Am J Kidney Dis* 40:1005–1012, 2002
22. Hayashi T, Era S, Kawai K, *et al*: Observation for redox state of human serum and aqueous humor albumin from patients with senile cataract. *Pathophysiology* 6:237–243, 2000
23. Climent I, Tsai L, Levine RL: Derivatization of gamma-glutamyl semialdehyde residues in oxidized proteins by fluoresceinamine. *Anal Biochem* 182:226–232, 1989
24. Schagger H, von Jagow G: Tricine-sodium dodecyl sulfate-polyacrylamide gel electrophoresis for the separation of proteins in the range from 1 to 100 kDa. *Anal Biochem* 166:368–379, 1987

25. Halliwell B, Gutteridge JM: The antioxidants of human extracellular fluids. *Arch Biochem Biophys* 280:1–8, 1990
26. Feri B, Stocker R, Ames BN: Small molecule antioxidant defenses in human extracellular fluids, in *The Molecular Biology of Free Radical Scavenging*, edited by Scandalios J, Cold Spring Harbor, Cold Spring Harbor Laboratory Press, 1992, pp 23–45
27. Berlett BS, Stadtman ER: Protein oxidation in aging, disease, and oxidative stress. *J Biol Chem* 272:20313–20316, 1997
28. Dean RT, Fu S, Stocker R, *et al*: Biochemistry and pathology of radical-mediated protein oxidation. *Biochem J* 324(Pt 1):1–18, 1997
29. Radi R, Beckman JS, Bush KM, *et al*: Peroxynitrite oxidation of sulfhydryls. The cytotoxic potential of superoxide and nitric oxide. *J Biol Chem* 266:4244–4250, 1991
30. Finch JW, Crouch RK, Knapp DR, *et al*: Mass spectrometric identification of modifications to human serum albumin treated with hydrogen peroxide. *Arch Biochem Biophys* 305:595–599, 1993
31. Soriani M, Pietraforte D, Minetti M: Antioxidant potential of anaerobic human plasma: Role of serum albumin and thiols as scavengers of carbon radicals. *Arch Biochem Biophys* 312:180–188, 1994
32. Stamler JS, Simon DI, Osborne JA, *et al*: S-nitrosylation of proteins with nitric oxide: Synthesis and characterization of biologically active compounds. *Proc Natl Acad Sci USA* 89:444–448, 1992
33. DeMaster EG, Quast BJ, Redfern B, *et al*: Reaction of nitric oxide with the free sulfhydryl group of human serum albumin yields a sulfenic acid and nitrous oxide. *Biochemistry* 34:11494–11499, 1995
34. Zhang H, Means GE: S-nitrosation of serum albumin: Spectrophotometric determination of its nitrosation by simple S-nitrosothiols. *Anal Biochem* 237:141–144, 1996
35. Gatti RM, Radi R, Augusto O: Peroxynitrite-mediated oxidation of albumin to the protein-thiyl free radical. *FEBS Lett* 348:287–290, 1994
36. Anraku M, Kragh-Hansen U, Kawai K, *et al*: Validation of the chloramine-T induced oxidation of human serum albumin as a model for oxidative damage in vivo. *Pharm Res* 20:684–692, 2003
37. Foley RN, Parfrey PS, Sarnak MJ: Clinical epidemiology of cardiovascular disease in chronic renal disease. *Am J Kidney Dis* 32:S112–S119, 1998
38. Bartfay WJ, Butany J, Lehotay DC, *et al*: A biochemical, histochemical, and electron microscopic study on the effects of iron-loading on the hearts of mice. *Cardiovasc Pathol* 8:305–314, 1999
39. Feldman HI, Santanna J, Guo W, *et al*: Iron administration and clinical outcomes in hemodialysis patients. *J Am Soc Nephrol* 13:734–744, 2002
40. Drueke T, Witko-Sarsat V, Massy Z, *et al*: Iron therapy, advanced oxidation protein products, and carotid artery intima-media thickness in end-stage renal disease. *Circulation* 106:2212–2217, 2002
41. Descamps-Latscha B, Witko-Sarsat V: Importance of oxidatively modified proteins in chronic renal failure. *Kidney Int* 59:108–113, 2001
42. Boaz M, Smetana S, Weinstein T, *et al*: Secondary prevention with antioxidants of cardiovascular disease in endstage renal disease (SPACE): Randomised placebo-controlled trial. *Lancet* 356:1213–1218, 2000
43. Roob JM, Khoschsorur G, Tiran A, *et al*: Vitamin E attenuates oxidative stress induced by intravenous iron in patients on hemodialysis. *J Am Soc Nephrol* 11:539–549, 2000

# Binding of $\alpha_1$-Acid Glycoprotein to Membrane Results in a Unique Structural Change and Ligand Release

Koji Nishi,[‡] Toru Maruyama,[‡] H. Brian Halsall,[§] Tetsuro Handa,[||] and Masaki Otagiri*[,‡]

*Graduate School of Pharmaceutical Science, Kumamoto University, 5-1 Oe-honmachi, Kumamoto 862-0973, Japan, Department of Chemistry, University of Cincinnati, Cincinnati, Ohio 45221-0172, and Graduate School of Pharmaceutical Sciences, Kyoto University, 46-29 Yoshida Shimoadachi-cho, Sakyo-ku, Kyoto 606-8501, Japan*

*Received March 31, 2004; Revised Manuscript Received May 25, 2004*

ABSTRACT: $\alpha_1$-Acid glycoprotein (AGP) consists of 183 amino acid residues and 5 carbohydrate chains and binds to basic and neutral drugs as well as steroid hormones. We investigated the structural properties and ligand-binding capacity of AGP under mild acidic conditions and its interactions with liposomes prepared from neutral or anionic lipids and the neutral drug, progesterone. Interestingly, AGP had a unique structure at pH 4.5, at which the tertiary structure changed, whereas the secondary structure remained intact. Furthermore, the binding capacity of AGP for progesterone did not significantly change under these conditions. It was also observed that AGP was strongly bound to the anionic membrane at pH 4.5, forming an α-helix-rich structure from the original β-sheet-rich structure, which significantly decreased the binding capacity of AGP for progesterone. The structural transitions as well as the membrane binding were suppressed by adding NaCl. These results indicate that AGP has a unique structure on the membrane surface under mild acidic conditions. The conformational change induces binding to the membrane aided by electrostatic interaction, and AGP subsequently takes on a predominantly α-helical conformation.

$\alpha_1$-Acid glycoprotein (AGP),[1] a member of the lipocalin family, is a polypeptide with two disulfide bonds and five carbohydrate chains, which account for about 40% of its total mass of 36 kDa (*1*). It is a major binding protein for neutral and basic ligands (*2*−*5*). Although the three-dimensional structure and biological functions are still unknown, circular dichroism measurements (*6*) and molecular modeling (*7*) have revealed that this protein has a largely β-sheet structure in aqueous solution.

The hypothesis that membrane transport of a drug depends on the nonbound drug concentration is widely accepted. However, because this hypothesis does not fully explain the uptake mechanism of some AGP-binding drugs, a protein-mediated uptake system has been proposed (*8*−*11*). In such a system, structural changes in the protein due to interaction with the membrane surface decrease the drug-binding capacity. The recent ESR spectroscopic finding that the structure of HSA changes after interaction with the surface of hepatocytes supports this proposed system (*12*). It was recently reported that AGP binds to the vascular endothelial cell surface and then causes transcytosis across the cell without passing the intercellular junction (*13*). Andersen detected AGP on the surface of human monocytes, granulocytes, and lymphocytes using fluorescent electron microscopy (*14*, *15*). Other studies of AGP interacting with vesicles (*16*) and liposomes (*17*) also support the conclusion that AGP interacts with the membrane in circulation and may influence intracellular events. Furthermore, the oligosaccharide moiety of AGP is recognized by cell surface lectins (*18*).

We previously reported that the interaction between AGP and a biomembrane model (reverse micelles) resulted in structural change and a decrease in ligand-binding capacity. Moreover, this interaction resulted in a unique conformational transition: β-sheet to α-helix (*19*). Based on these results, it is important to investigate the structural properties and ligand-binding capacity of AGP under mild acidic conditions because local changes in pH on the biomembrane surface influence these parameters (*20*). Indeed, there are several reports that proteins undergo structural and functional changes under mild acidic conditions on the membrane surface and intracellularly (*21*−*23*), including other lipocalins (*24*).

In the present paper, we examined the relationship between structural properties under mild acidic conditions and the ability of AGP to interact with phospholipid interfaces containing neutral and anionic phospholipids. We demonstrate that AGP undergoes a unique conformational change under mild acidic conditions and that this conformational change promotes an interaction with the membrane. The ligand is then released due to either a change in affinity or closer membrane association. The process is a potentially useful model for studying the pharmacokinetics of both endogenous and exogenous substance binding to AGP and for elucidating further functions of AGP.

* To whom correspondence should be addressed. Tel: 81-96 371-4150. Fax: 81-96 362-7690. E-mail: otagirim@gpo.kumamoto-u.ac.jp.
‡ Kumamoto University.
§ University of Cincinnati.
|| Kyoto University.

[1] Abbreviations: AGP, $\alpha_1$-acid glycoprotein; HSA, human serum albumin; PC, L-α-phosphatidylcholine; PG, L-α-phosphatidyl-DL-glycerol; PS, L-α-phosphatidyl-L-serine; PE, L-α-phosphatidyl ethanolamine; CD, circular dichroism; PAI-1, plasminogen activator inhibitor 1.

10.1021/bi0400204 CCC: $27.50 
Published on Web 07/22/2004

## MATERIALS AND METHODS

*Materials.* AGP (Cohn fraction VI), progesterone, L-α-phosphatidylcholine (PC) and ethanolamine (PE) from egg yolks, L-α-phosphatidyl-L-serine (PS) from bovine brain, and L-α-phosphatidyl-DL-glycerol sodium salt (PG) were all from Sigma Chemical Co. (St. Louis, MO). All other chemicals and solvents were of analytical grade.

*Liposome Preparation.* Liposomes were prepared as described previously (*25*). Briefly, phospholipids were dissolved in chloroform, and the solvent was evaporated under a stream of nitrogen and then under vacuum for at least 1 h. The phospholipid film was dispersed in the following 20 mM buffers: sodium phosphate (pH 6.0−7.4) and sodium acetate (pH 4.5−5.5), each containing 0−150 mM NaCl. Small unilamellar vesicles were prepared by sonication with a probe sonicator to near optical clarity, and residual multilamellar vesicles and titanium particles released from the probe were removed by centrifugation at 14000*g* for 20 min. Vesicles were mixed with AGP in the buffer at a final concentration of 10 mM AGP and 50−600 μM phospholipids (1:5−1:60 molar ratio of protein to phospholipids), and samples were incubated at room temperature for at least 1 h.

*Measurement of Circular Dichroism Spectra.* Circular dichroism spectra were recorded with a Jasco J-720 spectropolarimeter, using 10 μM AGP in 20 mM buffer (described above) at each pH. UV spectra were recorded in 10 mm and in 1 mm path length cells for near- and far-UV spectra, respectively.

*Measurement of Fluorescence Spectra.* Fluorescence was measured using a Jasco FP-770 fluorometer (Tokyo). AGP was dissolved at 10 μM in appropriate buffers. For Trp fluorescence, the excitation wavelength was 280 nm, and emission was monitored from 300 to 400 nm. ANS was added to a final concentration of 20 μM (2:1 molar ratio of ANS to AGP), which was enough to form the complex of AGP−ANS as much as possible and prevent nonspecific binding because it was reported that AGP had a high-affinity site for ANS (*25*). Spectra were recorded immediately after mixing. The excitation wavelength was 380 nm, and emission was monitored from 450 to 550 nm.

*Membrane-Binding Experiment.* Sucrose-loaded large unilamellar vesicles were prepared as previously described (*26*). The buffers (20 mM) used at each pH were as described above. Repeating the experiment with various buffers showed that the results depended on pH and not the buffer used. After incubation for 10 min at room temperature, solutions were centrifuged (20000*g*, 30 min) to separate vesicles and associated protein (pellet) from soluble protein (supernatant). Control experiments at all pH values showed that, in the absence of phospholipid vesicles, no AGP was present in the pellet after centrifugation. Samples were analyzed by the Bradford assay.

*Progesterone−AGP-Binding Experiment.* Binding of progesterone to AGP was determined by the ultrafiltration method. Progesterone was dissolved as 1 mg/mL in acetonitrile, and the stock solution was diluted with 20 mM sodium phosphate buffer (pH 6.0−7.4) and sodium acetate buffer (pH 4.5−5.5). The final concentration of acetonitrile did not exceed 1%. AGP solution (1 mL) containing progesterone was incubated for 10 min on ice and then centrifuged at 2000*g* for 40 min at 4 °C. After centrifugation, the filtrate (10 μL) was analyzed by HPLC to determine the free progesterone concentration. The HPLC system consisted of a Hitachi 655A-11 pump (Hitachi, Tokyo) and a Hitachi L-4000 UV detector set at 244 nm. The analytical column used was an AM312 ODS column (150 × 6.0 mm i.d., S-5 mm, 120 Å) (YMC, Kyoto) and was maintained at room temperature. The mobile phase was acetonitrile−20 mM sodium phosphate buffer (pH 7.4) (50:50 v/v) at a flow rate of 1 mL/min. AGP and PG concentrations were 10 and 400 μM, respectively. AGP−progesterone-binding experiments in the presence of liposomes had a final progesterone concentration of 10 μM (1:1 molar ratio of progesterone to AGP) after the liposomes had been saturated in progesterone to limit its nonspecific adsorption by the liposomes.

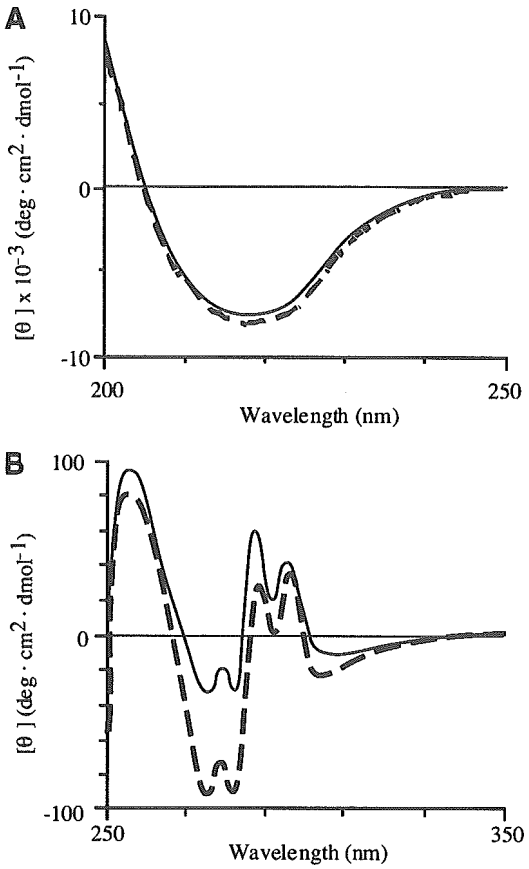


FIGURE 1: Effects of pH on the far-UV (A) and near-UV (B) CD spectra of AGP at pH 7.4 and 4.5, AGP spectra are shown as a continuous line (pH 7.4) and a dashed line (pH 4.5). Circular dichroism spectra were recorded using 10 μM AGP in a solution containing 20 mM buffer: sodium phosphate (pH 7.4) or sodium acetate (pH 4.5).

## RESULTS

*Effects of pH on the Conformational Structure of AGP.* It has been reported that the pH at the membrane surface is lowered due to the membrane potential (*20*). This pH decrease may mediate interactions between proteins and the membrane itself (*24*). We investigated how the tertiary and secondary structures of AGP were affected under mild acidic conditions (pH 4.5−6.5) using circular dichroism spectroscopy (Figure 1). The tertiary structure changed slightly compared with that at pH 7.4, but the secondary structure was unaffected, even at pH 4.5. To obtain more information about the conformational changes in AGP under mild acidic

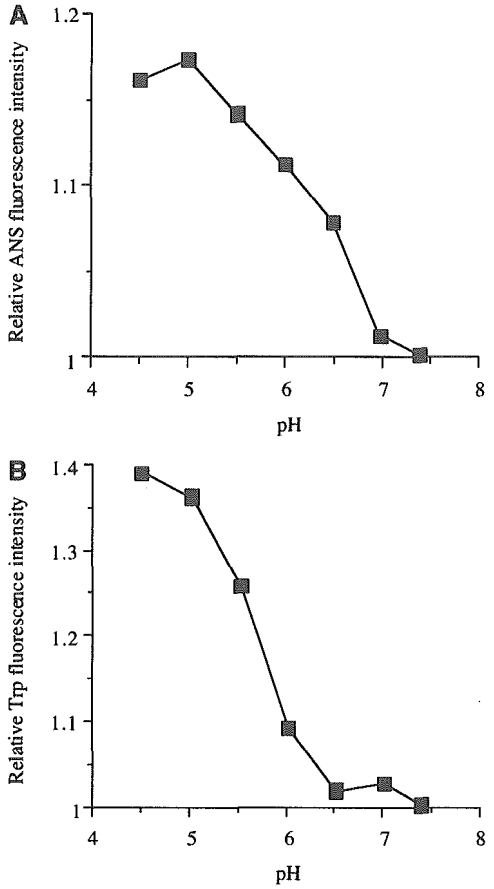


FIGURE 2: Fluorescence spectra of ANS and Trp residues at various pHs. AGP was dissolved at 10 $\mu$M in the appropriate buffers, and ANS was added to a final concentration of 20 $\mu$M (2:1 molar ratio of ANS to AGP). ANS: excitation wavelength, 380 nm; Trp: excitation wavelength, 280 nm.

conditions, we measured the fluorescence spectra of ANS and Trp residues on AGP at pH 4.5−7.4 (Figure 2). ANS is often used to evaluate hydrophobic regions, which are generally in the protein interior (*25*, *27*, *28*). The fluorescence intensity of ANS and Trp residues increased with lowering of pH. These results indicate that AGP has a unique conformational structure under the mild acidic conditions of the membrane surface, even in the absence of direct interactions between AGP and the membrane.

*Effects of pH and NaCl on the AGP−Membrane Binding.* The membrane environment has been shown to have a negative charge, in addition to being mildly acidic (*20*). We therefore examined the binding of AGP to PG- and PC-based membranes at each pH (pH 4.5−7.4) (Figure 3A). AGP bound strongly to the PG−membrane with lower pH, whereas significant binding was not observed with the PC−membrane at any pH. To confirm the presence of electrostatic forces in this interaction, the effects of NaCl on this binding were examined with the PG−membrane at pH 4.5 (Figure 3B). NaCl suppressed binding in a concentration-dependent manner (0 mM, 96.0 ± 0.58%; 75 mM, 37.5 ± 2.64%; and 150 mM, 10.0 ± 16.3%). The finding that other cations, $Ca^{2+}$ and $K^+$, also inhibited the interaction between AGP and membrane suggests the presence of electrostatic force (data not shown). The above interaction was also observed even in physiological buffer, but it was small, as expected from the NaCl effect. To test the validity of this model and

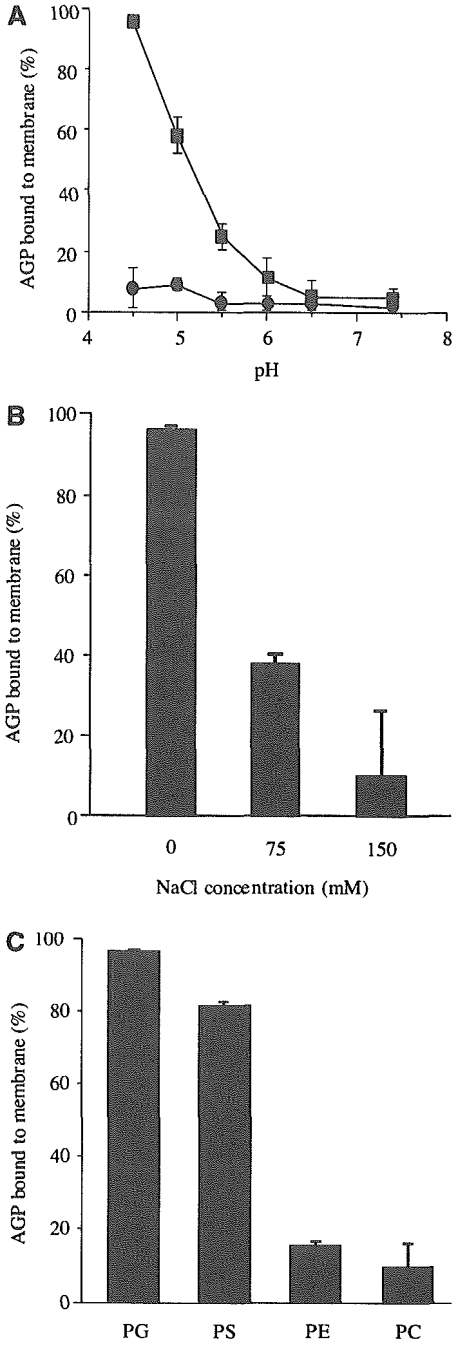


FIGURE 3: Interaction mode of AGP−membrane binding. (A) pH dependence of AGP binding to the membrane [PC (●), PG (■)]. (B) Effect of NaCl on the binding of AGP to the membrane. (C) Binding of AGP to the membrane made from other phospholipids. Experiments were performed using 10 $\mu$M AGP in solutions containing 20 mM buffers as described in Materials and Methods. Phospholipid vesicles were prepared at 400 $\mu$M.

experiment, the binding experiment was repeated using other phospholipids: PS and PE (Figure 3C). PG, PS, and PE (the degree of the negative charge: PG > PS > PE) are anionic lipids, PC is neutral, and the pattern of interaction of AGP with the lipids also supported the existence of an electrostatic interaction between AGP and the membrane. Moreover, at each pH, binding of AGP to PG−membrane had a significant correlation with the fluorescence intensity of Trp residues ($r = 0.9901$, $p < 0.01$) (Figure 4) but not ANS (data not shown). These results strongly suggest that the slight changes in AGP conformation observed under mild acidic conditions

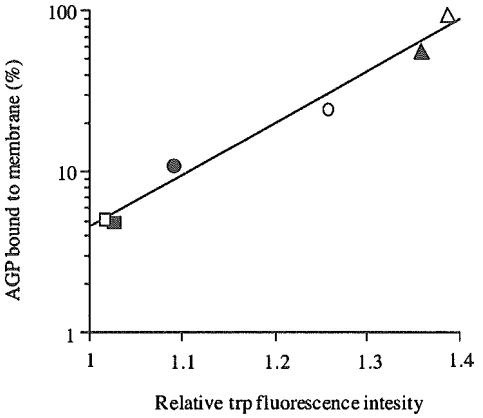


FIGURE 4: Correlation between AGP−membrane interaction and Trp residues of the AGP environment under mild acidic conditions. Each symbol represents the following pH: (■) 7.0, (□) 6.5, (●) 6.0, (○) 5.5, (▲) 5.0, and (△) 4.5.

lead to the binding of AGP to the membrane. This interaction may involve an electrostatic component.

*Effects of pH and NaCl on the Conformation of AGP in Membrane Interactions.* To evaluate the structural properties of AGP in membrane interactions, we examined the effects of pH and NaCl on the conformation of AGP in the presence of a PG−membrane (Figure 5). Panels B−D of Figure 5 show a $-[\theta]$ value of 222 nm as an index of the α-helix content. The secondary structure of AGP shifted from being β-sheet-rich to an α-helix-rich structure at lower pH (Figure 5A,B). In addition, the degree of this conformational transition depended on the PG concentration (Figure 5C) and was inhibited by higher NaCl concentrations (Figure 5D). These results indicated that this conformational transition was initiated following, or during, binding of AGP to the membrane.

*Effects of Ligand-Binding Capacity of AGP in Membrane Interaction.* It is important to understand how the ligand-binding capacity of AGP changes when the structural transition (β-sheet to α-helix) occurs in the presence of the PG−membrane. We used a representative AGP-binding ligand, progesterone, because it is uncharged and therefore unaffected by pH. The binding of progesterone to AGP had a good correlation with the α-helix content of AGP interacting with the PG−membrane at pH 4.5−7.4 ($r = 0.9545$, $p < 0.01$) (Figure 6). No changes in binding capacity were observed for pH 4.5−7.4 in the absence of PG−membrane. These results show that the binding of progesterone to AGP was strongly affected by its interaction with the PG−membrane but was not affected by mild acidic conditions.

## DISCUSSION

The hypothesis that uptake of a drug depends on the free drug concentration (not bound by protein) is widely accepted. However, a pharmacokinetic study using albumin- and AGP-binding ligands found that uptake is more efficient than predicted by this model (*8*). One explanation for this phenomenon is that structural changes in the carrier protein may be induced by interaction with the target cell surface. Consequently, the ligand is released concomitantly with conformational changes in the protein (*8*−*11*). This idea is supported by ESR spectroscopic findings showing that albumin undergoes structural changes when interacting with hepatocytes (*12*). It should also be noted that AGP binds to

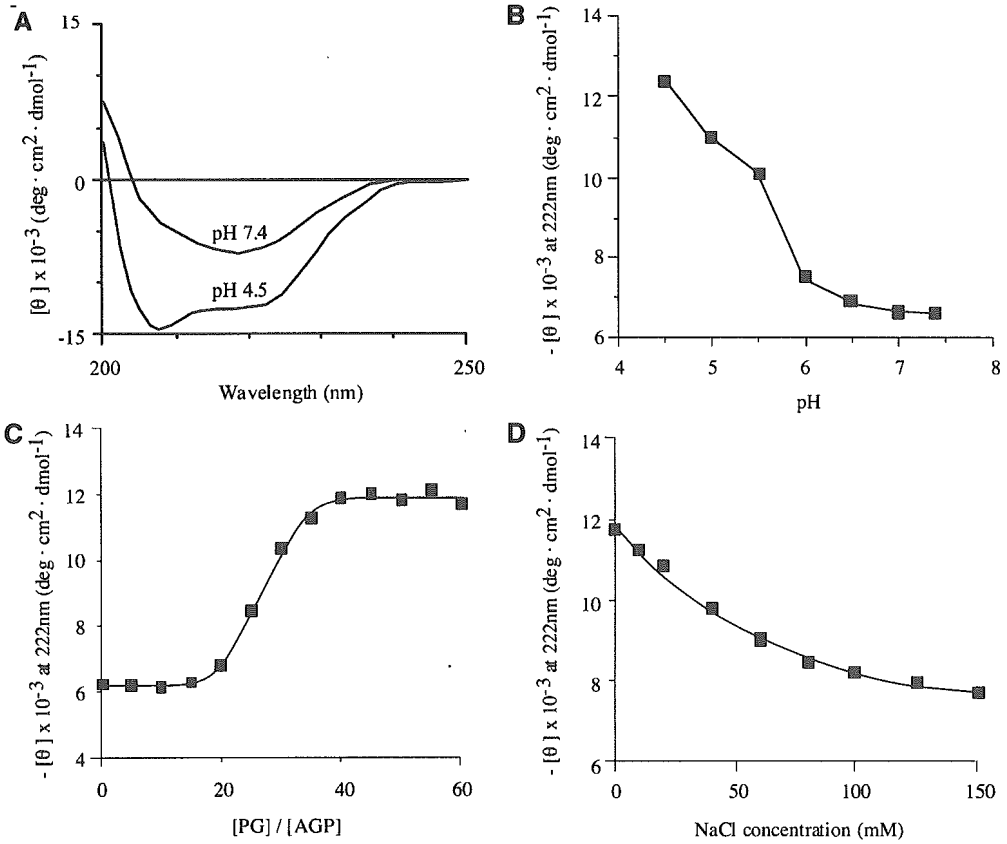


FIGURE 5: Effect of pH (A, B), PG concentration (C), and NaCl (D) on the conformational transition of AGP interacting with the membrane. Experiments were performed using 10 μM AGP in solution containing 20 mM buffer as described in Materials and Methods. The pH was 4.5 or 7.4 (A), was varied from 4.5 to 7.4 (B), or was 4.5 (C, D). Phospholipid vesicles were prepared at 400 μM (A, B, and D).

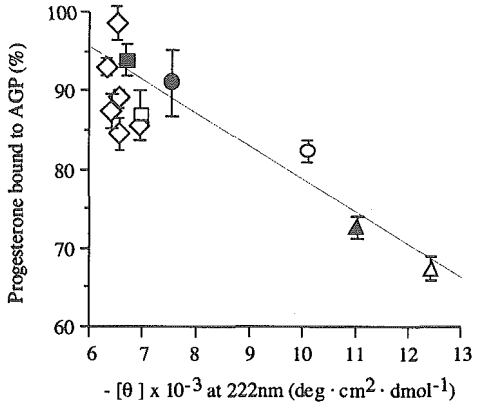


FIGURE 6: Binding of progesterone to AGP interacting with the membrane. AGP and PG concentrations were set at 10 and 400 $\mu$M, respectively. AGP–progesterone-binding experiments in the presence of liposomes were performed at a final progesterone concentration of 10 $\mu$M (1:1 molar ratio of progesterone to AGP) after liposomes were saturated in progesterone. The experiment was performed in a solution containing 20 mM appropriate buffer. Each symbol represents the following pH: (■) 7.0, (□) 6.5, (●) 6.0, (○) 5.5, (▲) 5.0, (△) 4.5, and (◇) 7.0–4.5 in the absence of PG–membrane.

vascular endothelial cell surfaces (*13*). pH-linked conformational transitions frequently reflect interactions of proteins with membranes. This is due to the fact that the membrane potential decreases the local pH as compared with the bulk of the solution (*29*). The difference in pH has been experimentally determined to be 1.6 pH units, and the calculated value reaches 2.7 pH units (*20*). We observed that the tertiary structure of AGP changed slightly but the secondary structure was conserved under acidic conditions. At pH 4.5, the ligand-binding capacity of AGP was almost equal to that at pH 7.4. These results show that the structure of the AGP-binding area for progesterone is retained, even at pH 4.5.

An increasing number of proteins, including transferrin (*21*), influenza hemagglutinin (*22*), and the lipocalins retinol-binding protein (*23*) and tear lipocalin (*24*), undergo pH-linked structural changes. Such conformational transitions may be physiologically significant, because they may mediate ligand release or membrane fusion. In the case of transferrin, translocation across membranes from the neutral pH of the bloodstream to the acidic intracellular environment leads to opening of the protein structure and the release of iron, apparently with active participation of the receptor (*21*), and tear lipocalin is postulated to deliver lipids at the tear–film interface by a pH-linked structural change (*24*). The unique structural changes in AGP, which were observed in this experiment, may be the first event in membrane interaction.

We examined the structural properties of AGP and its ligand-binding capacity in the membrane–water phase using liposomes, which are frequently used as a biomembrane model. It was observed that the α-helix content of AGP tended to increase in the presence of a PG–membrane under mild acidic conditions. This result supports the idea that the unique structural changes in AGP under mild acidic conditions induce interaction with the membrane. The results obtained from the ANS and Trp fluorescence experiment suggest that the interaction of AGP with the membrane under mild acidic conditions may be promoted by a slight change of conformation of AGP but not a greater exposure of the

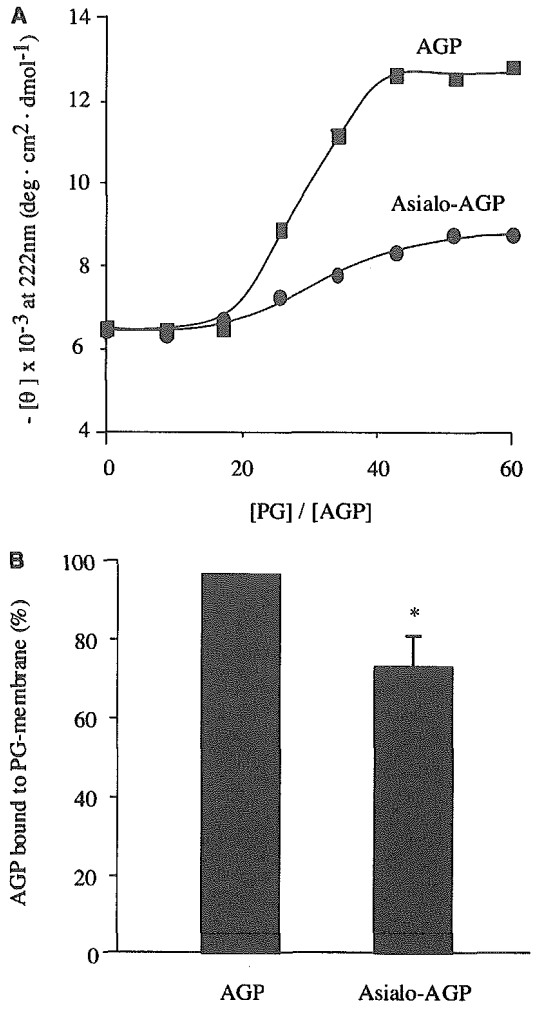


FIGURE 7: Effect of sialic acid on the interaction between AGP and PG–membrane. The degree of conformational transition of AGP (■) and asialo-AGP (●) interacting with PG–membrane (A) and the binding of AGP and asialo-AGP to PG–membrane (B) were monitored as in Figures 3 and 5.

hydrophobic side chains. When we examined the interactions of asialo-AGP with the anionic PG–membrane, the membrane-binding capacity and extent of the conformational transition both decreased at pH 4.5 (Figure 7). The finding that the conformational transition was decreased more than membrane binding may be due to an increase in the conformational stability of asialo-AGP. In accordance with this proposal, Friedman et al. have reported, by using fluorescence spectroscopy, that sequential removal of the sialic acids from AGP had no significant impact of the conformation of the protein core. However, the removal of sialic acids resulted in an increased stability of the core probably caused by interaction between the core and the asialoglycan chains (30). Aubert and Loucheux-Lefebvre also found by additive circular dichroism that the glycan chains do not perturb the protein core conformation (*6*). Villalobos et al. reported that the distribution of glycans on the AGP surface is asymmetric as found with monoclonal antibody probes (*31*), and Rojo-Dominguez and Hernandez-Arana and Schlueter predicted by molecular modeling that most of the glycans were distal to the proposed ligand-binding site (*7*, *32*). Together, these results strongly suggest that the influence of the terminal glycan sialic acid residues in the present work may be to orient the AGP at the PG–membrane surface and

present the relatively unprotected ligand-binding site to the membrane. Thus, it is likely that the initial conformational events that we observe in AGP involve residues that are present or closely coupled to those in the surface presented to the membrane.

In numerous proteins, insertion into the membrane seems to induce transition to an α-helix-rich structure (*33*−*38*). In the case of AGP, the ligand-binding area of AGP may involve regions that form an α-helix-rich structure and/or are inserted into the membrane since the $\lambda_{max}$ of Trp fluorescence was blue shifted due to interaction with the PG−membrane (pH 4.5, 340 nm; pH 4.5 + PG−membrane, 335.5 nm). Our preliminary experiment using the Trp mutants (W25A, W122A, and W160A) showed that Trp25 and Trp160 were inserted into the membrane.

Structural transitions similar to those found in AGP (α to β or β to α) have been observed in other proteins including β-lactoglobulin and plasminogen activator inhibitor (PAI-1) (*38*−*40*). For example, β-lactoglobulin readily changes to an α-helical structure from a β-sheet one, when exposed to more hydrophobic alcohol (e.g., trifluoroethanol) (*39*). We obtained similar results for AGP, containing for a series of alcohols an α-helix induction effect in AGP of propanol > ethanol > methanol (data not shown). These results suggest that hydrophobic interactions contribute to the formation of an α-helix on AGP observed in the presence of the membrane. The folding intermediate of PAI-1 (α-helix structure) is reportedly a functional state, while the native state is inert (*40*−*42*). Furthermore, a conformational transition from α-helix to β-sheet seems to induce propagation of prion proteins, resulting in prion diseases, such as bovine spongiform encephalopathy (*43*). It has also been reported that slight structural change of prion due to interaction with membrane might induce such a conformational transition (α-helix to β-sheet) (*44*).

The biological functions of AGP are currently unknown, although numerous activities have been described of which the most common is binding ligands, particularly therapeutic drugs. For example, AGP binds thalidomide and thereby affects the drug's immunomodulatory activity against tumor necrosis factor α (*45*). AGP is reportedly involved in intracellular events, such as controlling thrombocytic agglutinability, controlling bacterial englobement, extension during engrafting, and inhibiting lymphocyte growth through various mechanisms (*2*, *5*, *46*). AGP has been detected on the surface of normal human lymphocytes, granulocytes, and monocytes by fluorescent electron microscopy (*13*, *14*).

The limited data obtained here suggest that interaction between AGP and biomembranes may be important for other aspects of the physiological functions of this protein in addition to the observed changes in ligand-binding capacity.

## REFERENCES


1. Halsall, H. B., Austin, R. C., Dage, J. L., Sun, H., and Schlueter, K. T. (2000) Structural aspects of alpha1-acid glycoprotein and its interaction, in *Proceedings of the international symposium on serum albumin and alpha1-acid glycoprotein* (Otagiri, M., Sugiyama, Y., Testa, B., and Tillement, J. P., Eds.) pp 45−54, Tokyo Print, Kumamoto, Japan.
2. Kremer, J. M., Wilting, J., and Janssen, L. H. (1988) Drug binding to human alpha1-acid glycoprotein in health and disease, *Pharmacol. Rev. 40*, 1−47.
3. Treuheit, M. J., Costello, C. E., and Halsall, H. B. (1992) Analysis of the five glycosylation sites of human alpha1-acid glycoprotein, *Biochem. J. 283*, 105−112.
4. Clark, A. J., Clissold, P. M., Al Shawi, R., Beattie, P., and Bishop, J. (1984) Structure of mouse major urinary protein genes: different splicing configurations in the 3′-non-coding region, *EMBO J. 3*, 1045−1052.
5. Baumann, P., Muller, W. E., Eap, C. B., and Tillement, J. P. (1989) *Alpha1-acid glycoprotein. Genetics, biochemistry, physiological functions and pharmacology*, Alan R. Liss, New York.
6. Aubert, J. P., and Loucheux-Lefebvre, M. H. (1976) Carbohydrate-peptide linkage in glycoproteins, *Arch. Biochem. Biophys. 175*, 400−409.
7. Rojo-Dominguez, A., and Hernandez-Arana, A. (1993) Three-dimensional modeling of the protein moiety of human alpha1-acid glycoprotein, a lipocalin-family member, *Protein Sequences Data Anal. 5*, 349−355.
8. Lin, T. H., Sawada, Y., Sugiyama, Y., Iga, T., and Hanano, M. (1987) Effects of albumin and alpha1-acid glycoprotein on the transport of imipramine and desipramine through the blood-brain barrier in rats, *Chem. Pharm. Bull. 35*, 294−301.
9. Weisiger, R., Gollan, J., and Ockner, R. (1981) Receptor for albumin on the liver cell surface may mediate uptake of fatty acids and other albumin-bound substances, *Science 211*, 1048−1051.
10. Forker, E. L., and Luxon, B. A. (1981) Albumin helps mediate removal of taurocholate by rat liver, *J. Clin. Invest. 67*, 1517−1522.
11. Forker, E. L., and Luxon, B. A. (1983) Albumin-mediated transport of rose bengal by perfused rat liver. Kinetics of the reaction at the cell surface, *J. Clin. Invest. 72*, 1764−1771.
12. Horie, T., Mizuma, T., Kasai, S., and Awazu, S. (1988) Conformational change in plasma albumin due to interaction with isolated rat hepatocyte, *Am. J. Physiol. 254*, G465−G470.
13. Predescu, D., Predescu, S., McQuistan, T., and Palade, G. E. (1998) Transcytosis of alpha1-acidic glycoprotein in the continuous microvascular endothelium, *Proc. Natl. Acad. Sci. U.S.A. 95*, 6175−6180.
14. Andersen, M. M. (1983) Leucocyte-associated plasma proteins. Association of prealbumin, albumin, orosomucoid, alpha1-antitrypsin, transferrin and haptoglobin with human lymphocytes, monocytes, granulocytes and a promyelocytic leukaemic cell line (HL-60), *Scand. J. Clin. Lab. Invest. 43*, 49−59.
15. Andersen, M. M. (1984) Leucocyte-associated plasma proteins in leucocytes during disease states, and in leukaemic cells, *Scand. J. Clin. Lab. Invest. 44*, 257−265.
16. Cheresh, D. A., Haynes, D. H., and Distasio, J. A. (1984) Interaction of an acute phase reactant, alpha1-acid glycoprotein (orosomucoid), with the lymphoid cell surface: a model for non-specific immune suppression, *Immunology 51*, 541−548.
17. Neitchev, V. Z., and Bideaud, F. A. (1988) Temperature-dependent osmotic permeability in glycoprotein containing liposomes, *Mol. Biol. Rep. 13*, 85−88.
18. Drickamer, K. (1987) Membrane receptors that mediate glycoprotein endocytosis: structure and biosynthesis, *Kidney Int., Suppl. 23*, 167−183.
19. Nishi, K., Sakai, N., Komine, Y., Maruyama, T., Halsall, H. B., and Otagiri, M. (2002) Structural and drug-binding properties of alpha1-acid glycoprotein in reverse micelles, *Biochim. Biophys. Acta 1601*, 185−191.
20. van der Goot, F. G., Gonzalez-Manas, J. M., Lakey, J. H., and Pattus, F. (1991) A "molten-globule" membrane-insertion intermediate of the pore-forming domain of colicin A, *Nature 354*, 408−410.
21. Jeffrey, P. D., Bewley, M. C., MacGillivray, R. T., Mason, A. B., Woodworth, R. C., and Baker, E. N. (1998) Ligand-induced conformational change in transferrins: crystal structure of the open form of the N-terminal half-molecule of human transferrin, *Biochemistry 37*, 13978−13986.
22. Suren, A. T., and Lukas, K. T. (1996) Reversible pH-dependent conformational change of reconstituted influenza hemagglutinin, *J. Mol. Biol. 260*, 312−316.
23. Bychkova, V. E., Berni, R., Rossi, G. L., Kutyshenko, V. P., and Ptitsyn, O. B. (1992) Retinol-binding protein is in the molten globule state at low pH, *Biochemistry 31*, 7566−7571.
24. Gasymov, O. K., Abduragimov, A. R., Yusifov, T. N., and Glasgow, B. J. (1998) Structural changes in human tear lipocalins associated with lipid binding, *Biochim. Biophys. Acta 1386*, 145−156.

25. Essassi, D., Zini, R., and Tillement, J. P. (1990) Use of 1-anilino-8-naphthalene sulfonate as a fluorescent probe in the investigation of drug interactions with human alpha1-acid glycoprotein and serum albumin, *J. Pharm. Sci. 79*, 9−13.
26. Bruser, C. A., Signal, C. T., Resh, M. D., and McLaughlin, S. (1994) Membrane binding of myristylated peptides corresponding to the NH2 terminus of Src, *Biochemistry 33*, 13093−13101.
27. Muzammil, S., Kumar, Y., and Tayyab, S. (1999) Molten globule-like state of human serum albumin at low pH, *Eur. J. Biochem. 266*, 26−32.
28. Matthews, J. M., Norton, R. S., Hammacher, A., and Simpson, R. J. (2000) The single mutation Phe173 → Ala induces a molten globule-like state in murine interleukin-6, *Biochemistry 39*, 1942−1950.
29. McLaughlin, S. (1989) The electrostatic properties of membranes, *Annu. Rev. Biophys. Biophys. Chem. 18*, 113−136.
30. Friedman, M. L., Wermeling, J. R., and Halsall, H. B. (1986) The influence of *N*-acetylneuraminic acid on the properties of human orosomucoid, *Biochem. J. 236*, 149−153.
31. Halsall, H. B., Villalobos, A. P., Ivancic, J. S., Bencosme, A. I., and Chung, P. (1989) Monoclonal antibodies against human orosomucoid: tools for the exploration of structure, function and interactions, *Prog. Clin. Biol. Res. 300*, 67−84.
32. Schlueter, K. T. (1992) Photoaffinity labelling the basic binding site of orosomucoid, Ph.D. Dissertation, University of Cincinnati.
33. Kemmink, J., and Creighton, T. E. (1993) Local conformations of peptides representing the entire sequence of bovine pancreatic trypsin inhibitor and their roles in folding, *J. Mol. Biol. 234*, 861−878.
34. Ptitsyn, O. B. (1995) Molten globule and protein folding, *Adv. Protein Chem. 47*, 83−229.
35. London, E. (1992) Diphtheria toxin: membrane interaction and membrane translocation, *Biochim. Biophys. Acta 1113*, 25−51.
36. Gray, R. A., Vander Velde, D. G., Burke, C. J., Manning, M. C., Middaugh, C. R., and Borchardt, R. T. (1994) Delta-sleep-inducing peptide: solution conformational studies of a membrane-permeable peptide, *Biochemistry 33*, 1323−1331.
37. Jongh, H. H., Killian, J. A., and Kruijff, B. (1992) A water−lipid interface induces a highly dynamic folded state in apocytochrome *c* and cytochrome *c*, which may represent a common folding intermediate, *Biochemistry 31*, 1636−1643.
38. Banuelos, S., and Muga, A. (1995) Binding of molten globule-like conformations to lipid bilayers. Structure of native and partially folded alpha-lactalbumin bound to model membranes, *J. Biol. Chem. 270*, 29910−29915.
39. Hamada, D., Segawa, S., and Goto, Y. (1996) Non-native alpha-helical intermediate in the refolding of beta-lactoglobulin, a predominantly beta-sheet protein, *Nat. Struct. Biol. 3*, 868−873.
40. Mottonen, J., Strand, A., Symersky, J., Sweet, R. M., Danley, D. E., Geoghegan, K. F., Gerard, R. D., and Goldsmith, E. J.(1992) Structural basis of latency in plasminogen activator inhibitor-1, *Nature 355*, 270−273.
41. Berkenpas, M. B., Lawrence, D. A., and Ginsburg, D. (1995) Molecular evolution of plasminogen activator inhibitor-1 functional stability, *EMBO J. 14*, 2969−2977.
42. Boncela, J., Papiewska, I., Fijalkowska, I., Walkowiak, B., and Cierniewski, C. S. (2001) Acute phase protein alpha1-acid glycoprotein interacts with plasminogen activator inhibitor type 1 and stabilizes its inhibitory activity, *J. Biol. Chem. 276*, 35305−35311.
43. Prusiner, S. B. (1989) Scrapie prions, *Annu. Rev. Microbiol. 43*, 345−374.
44. Morillas, M., Swietnicki, W., Gambetti, P., and Surewicz, W. K. (1999) Membrane environment alters the conformational structure of the recombinant human prion protein, *J. Biol. Chem. 274*, 36859−36865.
45. Turk, B. E., Jiang, H., and Liu, J. O. (1996) Binding of thalidomide to alpha1-acid glycoprotein may be involved in its inhibition of tumor necrosis factor alpha production, *Proc. Natl. Acad. Sci. U.S.A. 93*, 7552−7556.
46. Bennett, M., and Schmid, K. (1980) Immunosuppression by human plasma alpha1-acid glycoprotein: importance of the carbohydrate moiety, *Proc. Natl. Acad. Sci. U.S.A. 77*, 6109−6113.

BI0400204

Available online at www.sciencedirect.com
SCIENCE DIRECT
Biochimica et Biophysica Acta 1702 (2004) 9–17
BIOCHIMICA ET BIOPHYSICA ACTA
BBA
www.bba-direct.com

# Stabilizing mechanisms in commercial albumin preparations: octanoate and *N*-acetyl-L-tryptophanate protect human serum albumin against heat and oxidative stress

Makoto Anraku[a], Yasufumi Tsurusaki[a], Hiroshi Watanabe[a], Toru Maruyama[a], Ulrich Kragh-Hansen[b], Masaki Otagiri[a,*]

[a]*Department of Biopharmaceutics, Graduate School of Pharmaceutical Sciences, Kumamoto University, 5-1 Oe-honmachi, Kumamoto 862-0973, Japan*
[b]*Department of Medical Biochemistry, University of Aarhus, DK-8000 Aarhus C, Denmark*

Received 17 May 2004; received in revised form 2 July 2004; accepted 13 July 2004
Available online 2 August 2004

**Abstract**

The capability of octanoate, *N*-acetyl-L-tryptophanate (*N*-AcTrp) and other ions of fatty acids and amino acids to stabilize human serum albumin (HSA) against thermal and oxidative stress was studied. Native-PAGE showed that octanoate, and more hydrophobic fatty acids anions, stabilizes the monomeric form of HSA during heating at 60 °C for 30 min. Heating in the presence of octanoate did not change the far-UV CD-spectrum. The stabilizing role of octanoate also showed as an increase in denaturation temperature and calorimetric enthalpy, determined by differential scanning calorimetry (DSC). *N*-AcTrp, which was found to compete with octanoate for a common high-affinity site, has only a minor stabilizing effect. By contrast, no effect was found for L-tryptophanate or *N*-acetyl-L-cysteinate. Any ligand effect on oxidation was examined by using 2,2′-azobis(2-amidino-propane)dihydrochloride (AAPH) as oxidizing agent. One hour of incubation resulted in the formation of the same number of carbonyl groups, whether octanoate or one of the abovementioned amino acids was present or not. However, the number of groups formed after 24 h of incubation was significantly decreased in the presence of L-tryptophanate and, especially, *N*-AcTrp. The effect of 1-h incubation with AAPH on the oxidative status of 34-Cys was studied by the HPLC technique. It was found that *N*-AcTrp, but not octanoate, has a large protecting effect on the sulfhydryl group. Thus, octanoate has the greatest stabilizing effect against heat, whereas the presence of *N*-AcTrp diminishes oxidation of HSA.


*Keywords:* Human serum albumin; Sulfhydryl group; Thermal stability; Antioxidant activity; Octanoate; *N*-Acetyl-L-tryptophanate

## 1. Introduction

Human serum albumin (HSA) is a single-chain, non-glycosylated polypeptide synthesized in and secreted from liver cells. According to X-ray crystallographic studies, it forms a heart-shaped protein having approximately 67% α-helix but no β-sheet [1,2]. A recent, combined phosphorescence depolarization-hydrodynamic modeling study proposed that the overall conformation of HSA in neutral solution is very similar to that observed in the crystal form [3]. The protein is composed of three homologous domains (I–III), and each domain has two subdomains (A and B) that possess common structural elements [1,2]. It has 35 cysteinyl residues, of which 34 form 17 stabilizing disulfide bridges. In mercaptalbumin (HMA) the last cysteine residue, at position 34, has a free SH group. However, in vivo part of the sulfhydryl groups is not free but forms a mixed disulfide with cysteine or glutathione (HNA-1) or undergoes oxidation (HNA-2) [4].

*Abbreviations:* HSA, human serum albumin; HMA, mercaptalbumin; HNA-1, albumin forming mixed disulfides; HNA-2, sulfhydryl-oxidized albumin; Oct, octanoate; *N*-AcTrp, *N*-acetyl-L-tryptophanate; L-Trp, L-tryptophanate; *N*-AcCys, *N*-acetyl-L-cysteinate; AAPH, 2,2′-azobis(2-amidino-propane)dihydrochloride; DSC, differential scanning calorimetry; CD, circular dichroism

* Corresponding author. Tel.: +81 96 371 4150; fax: +81 96 362 7690.
*E-mail address:* otagirim@gpo.kumamoto-u.ac.jp (M. Otagiri).

1570-9639/$ - see front matter © 2004 Elsevier B.V. All rights reserved.
doi:10.1016/j.bbapap.2004.07.002

HSA is the most abundant protein in plasma, and, in addition to being the chief colloid, it serves as an important transport and depot protein [5,6]. Huge amounts of albumin are used in the clinic during surgery and in the treatment shock trauma. Currently, the only source of HSA for clinical application is donated human blood. However, the risk of transmission of pathogenic vira such as those causing hepatitis, HIV, and others not yet identified exists. The vira usually are destroyed by heating at 60 °C for several hours. During this pasteurization process, sodium octanoate (Oct) and *N*-acetyl-L-tryptophanate (*N*-AcTrp) are widely used as stabilizers [6]. However, the mechanism of stabilization of these ligands is not fully elucidated. We used ultrafiltration to perform competition studies which showed that the two additives compete for the same high-affinity binding site, which most probably is placed in Sudlow's site II in subdomain IIIA [4]. Afterwards, we investigated the stabilizing effect of Oct, *N*-AcTrp and other fatty acid anions and amino acids by differential scanning calorimetry (DSC), circular dichroism (CD) and native-PAGE.

In plasma and in the interstitial fluid, HSA also functions as a major antioxidant [7]. Therefore, we also studied the protecting effect of the same ligands on oxidation of albumin. This was done by measuring protein-bound carbonyl groups and by investigating the contributions of HMA, HNA-1 and HNA-2 before and after oxidative stress. We found that the stabilizing effect of Oct against heat is superior to that of *N*-AcTrp, whereas the protecting effect of *N*-AcTrp against oxidation is much better than that of Oct.

## 2. Materials and methods

### 2.1. Materials

HSA was donated by Chemo-Sera-Therapeutic Research Institute (Kumamoto, Japan) and was defatted using charcoal treatment as described by Chen [8]. After dialysis against distilled water, the protein was freeze-dried and stored at −20 °C until use. *N*-Acetyl-L-tryptophan, L-tryptophan (L-Trp) and *N*-acetyl-L-cysteine (*N*-AcCys) were purchased from Nacalai Tesque (Kyoto, Japan). Fluoresceinamine (isomer II) as well as sodium salts of hexanoic acid, heptanoic acid, octanoic acid, nanoic acid, decanoic acid, undecanoic acid and dodecanoic acid were purchased from Sigma Chemical Co. (St. Louis, MO). [1-$^{14}$C]-Octanoic acid, sodium salt, was from Muromachi (Tokyo, Japan). 2,2′-Azobis(2-amidino-propane)dihydrochloride (AAPH) was purchased from Wako (Tokyo, Japan).

### 2.2. Determination of binding parameters for and interaction mode of Oct and N-AcTrp

Binding of Oct (2.5–40 μM) and *N*-AcTrp (1–100 μM) to HSA (40 μM) was determined by ultrafiltration using 67 mM sodium phosphate, pH 7.4 and 25 °C, as the buffer. Ultrafiltration was performed using 0.9-ml samples and an Amicon MPS-1 micropartition system with YMT ultrafiltration membranes (2000×*g*, 40 min). Ligand concentrations in the ultrafiltrate, representing free ligand concentrations ($C_f$), were determined by counting of radioactivity or HPLC. The concentration of Oct was determined by liquid-scintillation counting in a LSC-5000 from Aloka (Tokyo, Japan). The concentration of *N*-AcTrp was determined by the HPLC system, which consisted of a Hitachi 655A-11 pump and a Hitachi L-7480 type fluorescence detector. An Inertsil ODS-2 column (5 μM, 4.6×150 mm) was used as the stationary phase. The mobile phase consisted of 0.2 M acetate buffer (pH 4.5)–acetonitrile (75:25, v/v). The concentration was determined by using 280 and 360 nm as excitation and emission wavelengths, respectively.

For obtaining the relation between Oct concentration and radioactive counting, the radioactivity of the Oct-containing samples, with known total ligand concentration ($C_t$), was determined before ultrafiltration. Binding parameters were determined by fitting the experimental data to the following Scatchard equation using a nonlinear squares program (MULTI program).

$$r = \frac{C_b}{P_t} = \sum_{i=1}^{m} \frac{n_i K_i C_f}{1 + K_i C_f} \quad (1)$$

In this equation, $r$ is the average number of ligand molecules bound per molecule of protein, $n_i$ is the number of binding sites and $K_i$ is the corresponding association constant in the $i$th binding class. $P_t$ is the concentration of total protein, and the concentration of bound ligand ($C_b$) was calculated as $C_t - C_f$.

Two series of competition experiments with Oct and *N*-AcTrp were carried out. In the first series, the concentrations of total Oct (15 μM) and HSA (40 μM) were kept constant, whereas that of *N*-AcTrp varied from 1 to 100 μM. In the second series, the concentrations of total *N*-AcTrp (20 μM) and HSA (40 μM) were constant, whereas that of Oct varied from 2.5 to 40 μM.

Analysis of individual binding of Oct and *N*-AcTrp according to Eq. (1) revealed that both ligands bind to only one high-affinity site. In order to examine whether the ligands compete for the same site, the results of the competition experiments were analyzed according to the following general relationship.

$$r_A = \frac{K_A A_f}{1 + K_A A_f + K_B B_f} \quad (2)$$

In Eq. (2), $r_A$ is the average number of molecules of ligand A bound per molecule of albumin, $K_A$ and $K_B$ are the association constants for individual binding of ligand A and B, respectively, and $A_f$ and $B_f$ are the concentrations of the free forms of the ligands.

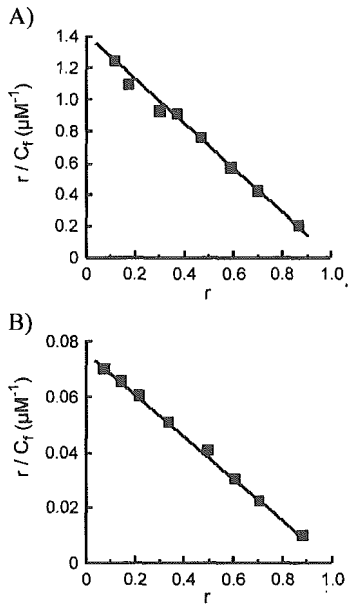


Fig. 1. Scatchard plots of the binding of Oct (A) and *N*-AcTrp (B) to HSA as determined by ultrafiltration. The results are average values for three experiments.

### 2.3. Effect of heating on HSA in the presence and absence of ligands

DSC was carried out on a MicroCal MC-2 ultrasensitive DSC (MicroCal Inc., Northampton, MA) using heating rates of 1 K/min. The protein concentration was 0.1 mM in 67 mM sodium phosphate buffer, pH 7.4. The calorimetric reversibility of the thermally induced transition was checked by reheating the protein solutions in the calorimetric cell, flushed with nitrogen, after cooling from the first run. The results showed, as also observed by Picó [9], that heating to or above 85 °C caused irreversible denaturation. The data obtained from DSC were applied to nonlinear fitting algorithms to calculate the thermodynamic parameters, thermal denaturation temperature ($T_m$), calorimetric enthalpy ($\Delta H_{cal}$) and van't Hoff enthalpy ($\Delta H_v$), from the temperature dependence of excess molar heat capacity, $C_p$, by employing Using Origin™ scientific plotting software.

Far-UV CD spectra (200–250 nm) were recorded with a Jasco J-720 spectropolarimeter (Tokyo, Japan) using a 1-mm path length cell. HSA (15 μM) was dissolved in 67 mM sodium phosphate buffer at pH 7.4 and 25 °C. The following four samples were prepared: (1) HSA alone, (2) HSA with Oct (75 μM), (3) HSA with *N*-AcTrp (75 μM), and (4) HSA with both ligands. CD spectra of the four samples were recorded without heating and after heating to 60 °C for 30 min.

Native-PAGE was run on Novex Tris–Glycine gels [10]. The following samples were used: HSA without and with preheating to 60 °C for 30 min, HSA preheated in the presence of *N*-AcTrp, *N*-AcTrp+Oct, Oct or other aliphatic fatty acid anions. The protein concentration was 24 μM and that of the additives was 120 μM. After incubation, aliquots were immediately mixed with cold native-PAGE sample buffer and loaded on the gel. As determined by a Bradford-assay [11,12], 10 μg of protein was added to each lane.

### 2.4. Effect of oxidation on HSA in the presence and absence of ligands

HSA, without and with additives, was oxidized by exposure to AAPH as described by Niki [13]. After incubation for 1 or 24 h, oxidation was stopped by adding acetone. Protein-bound carbonyl groups were quantitated using the method of Climent et al. [14]. In short, the groups were derivatized with fluoresceinamine and their number calculated from the absorbancy of the complexes at 490 nm (Jasco Ubest-35 UV/VIS spectrophotometer). During oxidation, the albumin concentration was 50 μM, and that of AAPH and any ligand was 10 mM and 250 μM, respectively. For both procedures, the medium was 67 mM sodium phosphate buffer, pH 7.4, 37 °C.

For another type of experiments, HSA, without and with additives, was oxidized by incubation with AAPH for 1 h. In order to separate HMA, HNA-1 and HNA-2, these samples were applied to an HPLC column. The column packing material, *N*-methylpyridinium polymer cross-linked with ethylene glycol dimethacrylate, was prepared as described

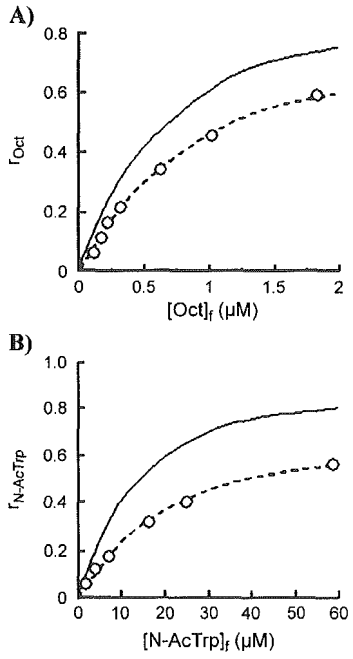


Fig. 2. (A) Binding of Oct to HSA in the presence of different concentrations of *N*-AcTrp (○). (B) Binding of *N*-AcTrp in the presence of different concentrations of Oct (○). The experimental data are average values for three determinations. The full curves represent independent ligand binding. The broken curves represent competitive binding of the ligands and were constructed using Eq. (2).

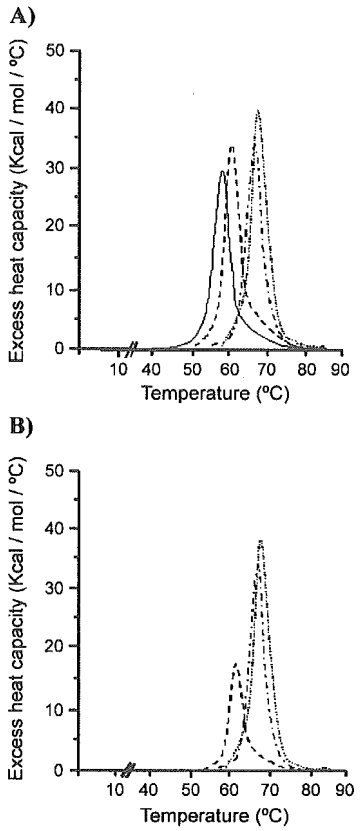


Fig. 3. Effect of Oct and *N*-AcTrp on the thermogram of HSA obtained from DSC measurements. (A) Curves for samples which have not been preheated. (B) Curves for samples which have been preheated for 30 min at 60 °C. Results are shown for HSA alone (——), HSA with *N*-AcTrp (– – –), HSA with Oct (– · –), and HSA with both ligands (- - - -). The curves are averages of three experiments.

previously [15,16]. The HPLC system also comprised of a Shimadzu LC-4A pump (Tokyo, Japan) equipped with a gradient programmer and a Shimadzu SPD-2AS UV monitor. Albumin was eluted with a 30-min linear gradient from 0 to 0.5 M sodium chloride in 0.05 M Tris–acetate buffer (pH 6.5, 25 °C) at a flow rate of 0.5 ml/min. Albumin was detected spectrophotometrically at 280 nm. The relative contributions of HMA, HNA-1 and HNA-2 were estimated by dividing the area of each fraction by the total area of HSA. During oxidation, which took place in media containing 67 mM sodium phosphate buffer (pH 7.4, 37 °C), the albumin concentration was 50 μM, and that of AAPH and any ligand was 10 mM and 250 μM, respectively.

## 3. Results and discussion

HSA used in the clinic, pharmaceutical-grade albumin, is pasteurized and delivered with Oct and *N*-AcTrp in molar ratios to albumin of approximately 5 to 1. In an attempt to facilitate the usefulness of the present information, we have solely used ligand–protein molar ratios of 5 to 1. Furthermore, the effects of prolonged heating were studied at 60 °C, and all experiments were carried out at physiological pH.

### *3.1. Binding of Oct and N-AcTrp to HSA*

First, we studied the individual binding of Oct and *N*-AcTrp. As seen in Fig. 1, a Scatchard analysis of the results obtained suggests the existence of one high-affinity binding site for both ligands. This suggestion was supported by analyzing the experimental data according to Eq. (1). $K_1$ for Oct was calculated as $1.3\pm0.2\times10^6$ $M^{-1}$ ($n$=3). Although Fig. 1A indicates that Oct only binds to a high-affinity site, the existence of secondary binding sites cannot be excluded. However, the affinity of these sites must be much lower than that of the primary site. The present $K_1$-value is in accordance with literature values [17]. $K_1$ for binding of *N*-AcTrp, which binds less strongly, was found to be $9.1\pm1.3\times10^4$ $M^{-1}$ ($n$=3). Also in this case, the existence of low-affinity, secondary binding cannot be excluded. The $K_1$-

Table 1
Thermodynamic data obtained from DSC of different HSA samples at pH 7.4[a]

| | Protein samples | $T_m$ (°C) | $\Delta H_{cal}$ ($10^2$ kcal/mol) | $\Delta H_v/\Delta H_{cal}$ |
|---|---|---|---|---|
| Without preheating | HSA | 59.19±0.05 | 1.61±0.10 | 1.0±10.01 |
| | HSA+Oct | 66.83±0.06 | 2.10±0.015 | 0.7±0.01 |
| | HSA+*N*-AcTrp | 62.05±0.10 | 1.61±0.05 | 1.1±0.03 |
| | HSA+Oct+n-AcTrp | 67.30±0.15 | 2.40±0.09 | 0.06±0.01 |
| | HSA+L-Trp | 61.10±0.12 | 1.60±0.06 | 1.0±0.01 |
| | HSA+*N*-AcCys | 59.69±0.015 | 1.75±0.05 | 1.0±0.02 |
| With preheating[b] | HSA | ND[c] | ND | ND |
| | HSA+Oct | 66.80±0.04 | 2.10±0.019 | 0.7±0.01 |
| | HSA+*N*-AcTrp | 62.43±0.05 | 0.87±0.25 | 1.8±0.01 |
| | HSA+Oct+n-AcTrp | 67.30±0.05 | 2.10±0.25 | 0.08±0.02 |
| | HSA+L-Trp | ND | ND | ND |
| | HSA+*N*-AcCys | ND | ND | ND |

[a] The concentration of HSA was 0.1 mM, and that of the ligands was 0.5 mM. The results are average values±S.D. for three experiments.
[b] Preheating was incubation at 60 °C for 30 min.
[c] No normal thermogram could be detected.

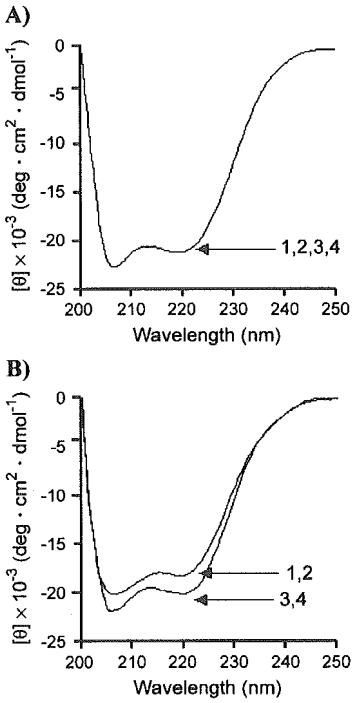


Fig. 4. Effect of Oct and *N*-AcTrp on the far-UV CD spectrum of HSA without (A) and with heat treatment for 30 min at 60 °C (B). (1) HSA alone, (2) HSA with *N*-AcTrp, (3) HSA with Oct, (4) HSA with both additives. The curves are averages of three experiments.

value is comparable to that ($1.9\times10^5$ $M^{-1}$) given in the classical paper of McMenamy and Oncley [18].

Displacement studies were performed in order to investigate the relation between high-affinity binding of Oct and *N*-AcTrp. Fig. 2 shows that binding of Oct at low *r*-values is diminished by the presence of *N*-AcTrp (Fig. 2A), and vice versa (Fig. 2B). An analysis using Eq. (2) proposes the presence of a common high-affinity binding site for the two ligands. This site seems to be placed in Sudlow's site II in subdomain IIIA [4,17].

### *3.2. Effect of heating on HSA in the presence and absence of ligands*

#### *3.2.1. DSC studies*

The stabilizing effect of Oct, *N*-AcTrp and other ligands on HSA was examined using different methods. First, we investigated the effect of Oct and *N*-AcTrp on the thermogram of HSA as determined by DSC. The results obtained for HSA, which has not been preheated, is shown in Fig. 3A. It is seen that addition of the ligands shifts the thermogram towards higher temperature as follows: Oct+*N*-AcTrp>Oct>*N*-AcTrp>HSA alone. Fig. 3B shows the results obtained after preheating the four protein samples. In this case, due to denaturation, no normal thermogram was obtained for HSA alone. However, addition of ligand protected albumin during preheating, and these samples resulted in thermograms which were shifted towards higher temperatures in the same order as illustrated in Fig. 3A. It is seen that the endotherms are single and sharp peaks indicating that thermal denaturation can be explained by a single component model [9,19]. Therefore, single values for $T_m$, $\Delta H_{cal}$ and $\Delta H_v$ can be calculated (Table 1).

The denaturation temperature, $T_m$, for HSA alone is almost the same as that (59.65 °C) published by Kosa et al. [19]. $T_m$ increases by adding ligands in the following order: Oct+*N*-AcTrp>Oct>*N*-AcTrp. The enthalpy change, $\Delta H_{cal}$, is generally thought to be due to the hydration of hydrophobic regions, buried in the native protein structure, during the unfolding process. Also this value (Table 1) is similar to that (166.3 kcal/mol) previously published [19].

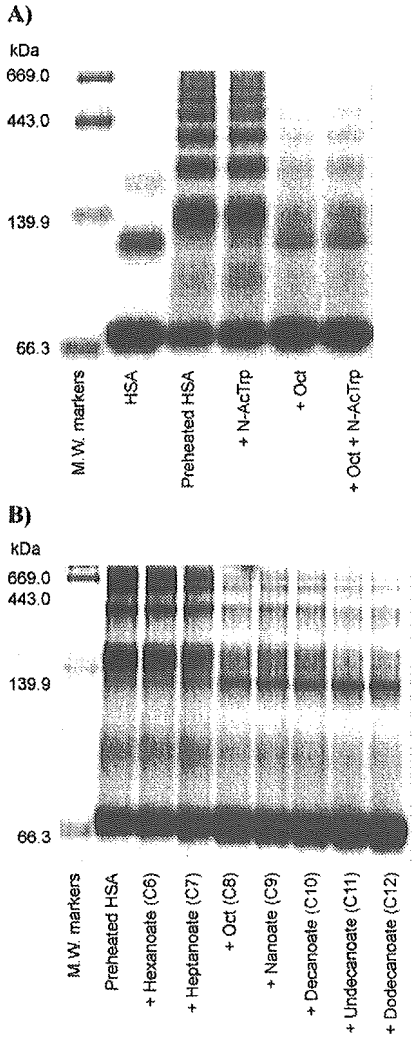


Fig. 5. Effect of heating for 30 min at 60 °C and of different ligands on the electrophoretic mobility of HSA. The concentration of polyacrylamide was 10% (A) or 12.5% (B). The gels were stained with Coomassie brilliant blue and then scanned. The figure shows representative experiments.

The $\Delta H_{cal}$-values varied in the same way as found for the $T_m$-values. If HSA was preheated for 30 min at 60 °C, followed by cooling, before the DSC-experiment, then no ordinary thermogram could be registered, indicating irreversible denaturation during preheating. By contrast, Oct and/or *N*-AcTrp was able to protect the protein during preheating. DSC analysis of the Oct-containing samples resulted in $T_m$- and $\Delta H_{cal}$-values which were comparable to those obtained without preheating (Table 1). In the presence of *N*-AcTrp alone, $T_m$ increased and $\Delta H_{cal}$ decreased somewhat as compared with the situation before heating.

The effect of other amino acids was also studied, namely L-Trp and *N*-AcCys. High-affinity binding of L-Trp most probably takes place, although with a lower affinity, to the same site as Oct and *N*-AcTrp [17], whereas *N*-AcCys interacts covalently with the thiol group of 34-Cys [4]. Addition of L-Trp or *N*-AcCys results in slightly higher $T_m$- and $\Delta H_{cal}$-values, comparable to those calculated for *N*-AcTrp addition. However, in contrast to *N*-AcTrp, L-Trp and *N*-AcCys have no protective effect during preheating.

The ratio of $\Delta H_v/\Delta H_{cal}$ is an index of the transition process to the denaturation states of proteins during thermal denaturation [19]. The values calculated for the preheated samples having Oct are almost the same as those calculated for the unheated samples, whereas that of the *N*-AcTrp containing sample is increased.

Shrake et al. [20] also found Oct to be more effective than *N*-AcTrp in protecting HSA against thermal denaturation. However, the thermograms of these authors exhibited two endotherms. The reason for this finding probably is that they used undefatted HSA, having 1.5 mol endogenous long-chain fatty acids anions per mole of protein, and a high salt concentration (145 mM NaCl). Likewise, Arakawa and Kita [21], using undefatted bovine serum albumin, observed that Oct has a greater protection against heat stress than *N*-AcTrp. In this case, the superior effect of Oct could not be fully explained by a larger increment of the melting temperature; $\Delta H_{cal}$ was not determined. It is also possible that the superior effect of Oct is ascribed to other mechanisms such as a synergy between the effects of bound fatty acids and *N*-AcTrp.

### 3.2.2. CD spectra and native-PAGE

Fig. 4 shows the effect of Oct and *N*-AcTrp on the far-UV CD spectrum of albumin without and with heating. As seen in Fig. 4A, HSA alone and in the presence of ligand, without preheating the samples, give indistinguishable spectra. From these spectra, an α-helical content of 66.2±2.1% ($n$=12) could be calculated. Heating of HSA with Oct or with both additives for 30 min has only a small diminishing effect on the CD spectrum (Fig. 4B). In these cases, the α-helical contents were calculated as 65.2±2.2% ($n$=3) and 66.4±1.7% ($n$=3), respectively. By contrast, *N*-AcTrp has no protective effect, because heating of HSA alone or in the presence of *N*-AcTrp results in similar and higher $\theta$-values, representing α-helical contents of 52.8±2.1% ($n$=3) and 54.9±1.4% ($n$=3), respectively. These results indicate that Oct is a better stabilizer than *N*-AcTrp.

Fig. 5 examines the effect of heating and of different ligands on the polymerization of HSA using native-PAGE. Fig. 5A shows that preheating of HSA in the absence of

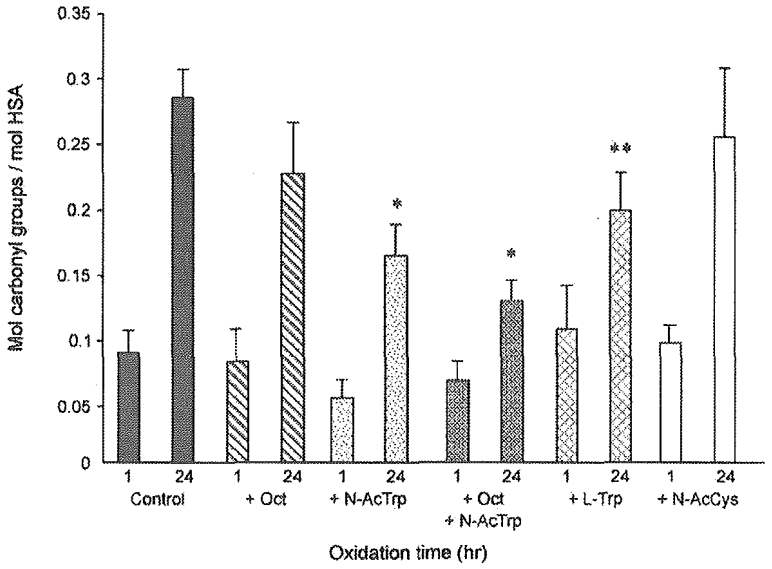


Fig. 6. AAPH-induced oxidation of HSA alone (control) and in the presence of ligands. The values are means±S.D.($n$=4). *$P$<0.01 and **$P$<0.05 as compared with control.

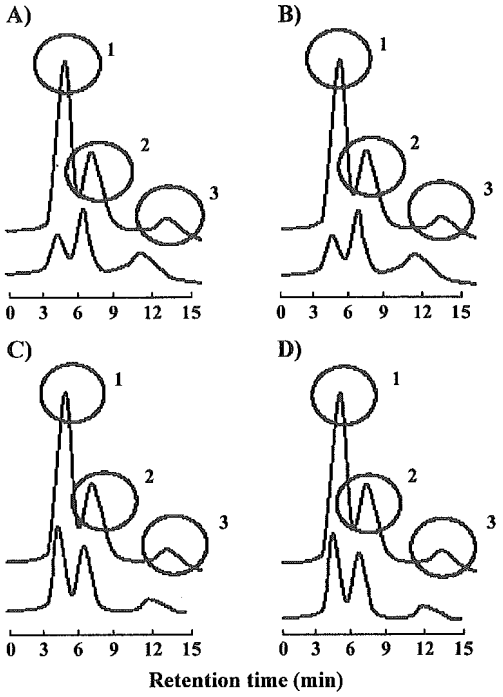


Fig. 7. HPLC chromatograms of HSA before (upper curves) and after AAPH-induced oxidation (lower curves). (A) Oxidation of albumin without ligands; (B) oxidation in the presence of Oct; (C) oxidation in the presence of *N*-AcTrp; (D) oxidation in the presence of both ligands. The peaks represent HMA (1), HNA-1 (2) and HNA-2 (3).

additives results in a very pronounced aggregation of the protein (lane 3 versus lane 2). The presence of *N*-AcTrp during preheating has no effect on aggregation (lane 4), whereas Oct alone or together with *N*-AcTrp has a pronounced diminishing effect on polymerization (lanes 5 and 6, respectively). Using undefatted bovine serum albumin, Arakawa and Kita [21] observed that both Oct and *N*-AcTrp prevented the heat-induced formation of albumin polymers. However, these effects could be due to the presence of albumin-bound endogenous, long-chain fatty acid anions.

Fig. 5B illustrates the effect of aliphatic fatty acid anions of different chain lengths. It is seen that hexanoate and heptanoate have no protecting effect (lanes 3 and 4, respectively, versus lane 2). By contrast, Oct and other additives of longer chain length have comparable protecting effects during preheating (lanes 5–9). Thus, the results reveal that the presence of a fatty acid having a chain length greater than seven carbon atoms is important for preventing excess polymerization during pasteurization. Among the candidates, Oct is the most convenient to use, because it has the highest solubility in aqueous media.

### *3.3. Effect of oxidation on HSA in the presence and absence of ligands*

HSA was exposed to AAPH, which oxidizes histidine, tryptophan, tyrosine and methionine residues in proteins [22]. Among other things, this results in the formation of carbonyl groups. The carbonyl content of HSA, which has not been exposed to AAPH, is 0.037±0.002 mol/mol protein ($n$=3) [23]. From Fig. 6, it is seen that this number increases with incubation time (control). It is also seen that the presence of the additives has no inhibiting effect on the carbonyl formation after 1-h exposure to AAPH, because no significant changes in carbonyl content were observed when compared to control. By contrast, some of the ligands have a protective effect during prolonged exposure to the oxidant. Thus, the presence of *N*-AcTrp results in a highly significant decrease in carbonyl groups. The protection against oxidation is even more evident, when both *N*-AcTrp and Oct are present, but this effect is mainly due to the presence of *N*-AcTrp, because addition of Oct alone gives no significant protection. Interestingly, the presence of L-Trp also reduces the number of carbonyl groups to a significant extent. By contrast, *N*-AcCys, which does not bind to site II, has no protective effect.

HSA is synthesized with a free sulfhydryl group at 34-Cys. However, in vivo, a major part of the group is either bound to free cysteine or glutathione (HNA-1) or oxidized to sulfenic, sulfinic or sulfonic states (HNA-2) [4]. In this study, we also investigated whether AAPH-treatment for 1 h affects the status of the SH-group of 34-Cys. From Fig. 7A, it is seen that native HSA mainly consists of HMA, with minor contributions of HNA-1 and HNA-2. A quantitative

Table 2
Relative fractions of HMA, HNA-1 and HNA-2 (%) before and after oxidation by AAPH[a]

| | | HSA alone | +Oct | +*N*-AcTrp | +Oct+*N*-AcTrp |
|---|---|---|---|---|---|
| Before oxidation | HMA | 65.1±2.3 | 66.1±2.9 | 65.3±2.5 | 65.3±2.5 |
| | HNA-1 | 22.8±2.5 | 23.4±4.2 | 21.5±3.5 | 22.5±3.7 |
| | HNA-2 | 10.6±5.3 | 10.8±4.5 | 11.6±4.5 | 11.5±5.4* |
| After oxidation | HMA | 22.3±2.8 | 22.3±2.5 | 39.3±2.3* | 39.2±2.6* |
| | HNA-1 | 51.4±2.5 | 51.3±4.2 | 45.3±3.1* | 45.6±3.4* |
| | HNA-2 | 26.7±5.3 | 26.5±4.5 | 13.5±4.5* | 15.5±5.5* |

[a] The concentration of HSA was 50 μM, and that of AAPH and ligands was 10 mM and 250 μM, respectively. The results are average values±S.D. for three experiments.

* $P$<0.05 as compared with HAS alone.